



Surface modification of inorganic nanoparticles for development of organic–inorganic nanocomposites—A review



Sarita Kango^a, Susheel Kalia^{b,c,*}, Annamaria Celli^b, James Njuguna^d, Youssef Habibi^e, Rajesh Kumar^a

^a Department of Physics and Materials Science, Jaypee University of Information Technology, Waknaghat 173234, Dist. Solan, H.P., India

^b Department of Civil, Chemical, Environmental and Materials Engineering, University of Bologna, Via Terracini 28, 40131 Bologna, Italy

^c Department of Chemistry, Bahra University, Waknaghat (Shimla Hills) 173234, Dist. Solan, H.P., India

^d School of Applied Sciences, Cranfield University, Cranfield, Bedford MK43 0AL, United Kingdom

^e Laboratory of Polymeric & Composite Materials, University of Mons, Place du Parc, 20 B-7000 Mons, Belgium

ARTICLE INFO

Article history:

Received 13 August 2012

Received in revised form 20 February 2013

Accepted 25 February 2013

Available online 7 March 2013

Keywords:

Inorganic nanoparticles

Surface modification

Grafting

Silane coupling agent

Organic–inorganic nanocomposites

ABSTRACT

Nanoparticles and nanocomposites are used in a wide range of applications in various fields, such as medicine, textiles, cosmetics, agriculture, optics, food packaging, optoelectronic devices, semiconductor devices, aerospace, construction and catalysis. Nanoparticles can be incorporated into polymeric nanocomposites. Polymeric nanocomposites consisting of inorganic nanoparticles and organic polymers represent a new class of materials that exhibit improved performance compared to their microparticle counterparts. It is therefore expected that they will advance the field of engineering applications. Incorporation of inorganic nanoparticles into a polymer matrix can significantly affect the properties of the matrix. The resulting composite might exhibit improved thermal, mechanical, rheological, electrical, catalytic, fire retardancy and optical properties. The properties of polymer composites depend on the type of nanoparticles that are incorporated, their size and shape,

Abbreviations: ABS, Acrylonitrile butadiene styrene; AIBN, 2,2'-azobisisobutyronitrile; AM, Acrylamide; APS, Aminopropyltrimethoxysilane; APTES, 3-aminopropyltriethoxysilane; APTMS, 3-aminopropyltrimethoxysilane; ATCC, American-type culture collection; BA, Butyl acrylate; CLIO, Crosslinked iron oxide nanoparticles; CTE, Coefficient of thermal expansion; DBSA, Dodecylbenzene sulfonic acid; DMA/DMTA, Dynamic-mechanical analysis /Dynamic mechanical thermal analysis; DNA, Deoxyribonucleic acid; DSC, Differential scanning calorimetry; DTA, Differential thermal analysis; GC, Glycol chitosan; HDA, Hexadecylamine; ICP-MS, Inductively coupled plasma mass spectrometry; IPTMS, 3-Isocyanatopropyltrimethoxysilane; LEDs, Light-emitting diodes; LLDPE, Linear low density polyethylene; MAA, Methacrylic acid; MION, Monocrystalline iron oxide nanoparticles; MMA, Methyl methacrylate; MNPs, Magnetic nanoparticles; MPC, 2-methacryloyloxyethyl phosphorylcholine; MPS, 3-(trimethoxysilyl)propyl methacrylate; MRI, Magnetic resonance imaging; Ms, Saturation magnetization; MTX, Methotrexate; NMR, Nuclear magnetic resonance; NPs, Nanoparticles; OA, Oleic acid; PA 6,6, Polyamide 6,6; PAAM, Polyacrylamide; PANi, Polyaniline; PBA, Polybutylacrylate; PC, Polycarbonate; PCEs, Power conversion efficiencies; PCL, Polycaprolactone; PCL-g-AA, Acrylic acid grafted polycaprolactone; PEG, Polyethylene glycol; PEGMA, Polyethylene glycol methacrylate; PEN, Poly(ethylene 2,6-naphthalate); PET, Polyethylene terephthalate; PHEA, Poly(hydroethyl acrylate); P3HT, Poly(3-hexylthiophene); PI, Polyimide; PINCs, Polymer inorganic nanocomposites; PMMA, Poly(methyl methacrylate); PP, Polypropylene; PPG, Poly(propylene glycol); PPGMA, Poly(propylene glycol) methacrylate; PPS, Polyphenylene sulphide; PPy, Polypyrrole; PS, Polystyrene; PTES, n-propyltriethoxysilane; PU, Polyurethane; PVA, Poly(vinylalcohol); PVP, Polyvinyl pyrrolidone; QDs, Quantum dots; RI, Refractive index; RNA, Ribonucleic acid; SI-ATRP, Surface-initiated atom transfer radical polymerization; SMA, Styrene-maleic anhydride copolymer; Spp, Syndiotactic polypropylene; SPR, Surface plasmon resonance; TEM, Transmission electron microscopy; TEOS, Tetraethoxysilane; TG, Glass transition; TGA, Thermogravimetric analysis; TGA-MS, Thermogravimetric analysis-mass spectrometry; THF, Tetrahydrofuran; TLIRP, Thiol-lactam initiated radical polymerization; TMA, Thermomechanical analysis; TOPO, Trioctylphosphine oxides; TTIP, Tetra isopropyl ortho titanate; UV, Ultra violet; VTES, Triethoxyvinylsilane.

* Corresponding author at: Department of Chemistry, Bahra University, Waknaghat 173234, Dist. Solan, H.P., India. Tel.: +91 9418604948; fax: +91 1792 247462.

E-mail addresses: susheel.kalia@gmail.com, susheel.kalia@yahoo.com (S. Kalia).

their concentration and their interactions with the polymer matrix. The main problem with polymer nanocomposites is the prevention of particle aggregation. It is difficult to produce monodispersed nanoparticles in a polymer matrix because nanoparticles agglomerate due to their specific surface area and volume effects. This problem can be overcome by modification of the surface of the inorganic particles. The modification improves the interfacial interactions between the inorganic particles and the polymer matrix. There are two ways to modify the surface of inorganic particles. The first is accomplished through surface absorption or reaction with small molecules, such as silane coupling agents, and the second method is based on grafting polymeric molecules through covalent bonding to the hydroxyl groups existing on the particles. The advantage of the second procedure over the first lies in the fact that the polymer-grafted particles can be designed with the desired properties through a proper selection of the species of the grafting monomers and the choice of grafting conditions.

© 2013 Elsevier Ltd. All rights reserved.

Contents

1. Introduction	1233
2. Inorganic nanoparticles.....	1235
2.1. Synthesis, properties and applications of selected inorganic nanoparticles	1235
3. Surface modification of inorganic nanoparticles	1236
3.1. Chemical treatments	1236
3.2. Grafting of synthetic polymers	1236
3.3. Ligand exchange technique	1239
3.4. Other methods of surface modification.....	1240
4. Applications of modified inorganic nanoparticles	1240
4.1. Dispersion of surface modified nanoparticles in organic solvents	1240
4.2. Photocatalytic and antibacterial applications	1242
4.3. Biomedical applications of surface modified nanoparticles.....	1243
4.4. Removal of heavy metal ions	1244
5. Organic–inorganic nanocomposite materials	1244
5.1. Methods of synthesis.....	1245
5.1.1. Sol-gel processing	1245
5.1.2. In situ polymerization	1245
5.1.3. Blending	1245
5.1.4. In situ growth of nanoparticles in a polymer matrix	1246
5.2. Properties of organic–inorganic nanocomposites	1247
5.2.1. Mechanical properties	1247
5.2.2. Optical properties	1249
5.2.3. Magnetic properties.....	1251
5.2.4. Electrical properties.....	1251
5.2.5. Thermal properties	1251
5.3. Applications of organic–inorganic nanocomposites.....	1252
6. Conclusions	1253
References	1253

1. Introduction

Development of organic–inorganic nanocomposites, often achieved by grafting synthetic polymers on inorganic particles or by adding modified nanoparticles (NPs) into polymer matrices, is intended to produce composite materials with improved mechanical and other properties. Nanocomposites made up of inorganic nanoparticles and organic polymers represent a new class of materials that exhibit improved performance when compared with their microparticle counterparts [1]. Surface modification of inorganic nanoparticles has attracted a great deal of attention because it produces excellent integration and an improved interface between nanoparticles and polymer matrices [2–5].

Polymer matrices reinforced with modified inorganic nanoparticles combine the functionalities of polymer matrices, which include low weight and easy formability, with the unique features of the inorganic nanoparticles. The nanocomposites obtained by incorporation of these types of materials can lead to improvements in several areas, such as optical, mechanical, electrical, magnetic, rheological, and fire retardancy properties [6,7]. However, the nanoparticles have a strong tendency to undergo agglomeration followed by insufficient dispersal in the polymer matrix, degrading the optical and mechanical properties of the nanocomposites [8,9]. To improve the dispersion stability of nanoparticles in aqueous media or polymer matrices, it is essential that the particle surface modification involving polymer surfactant molecules or other

Table 1

Synthesis, properties and applications of selected inorganic nanoparticles.

Sr. No.	Nanoparticle	Synthesis	Properties	Applications	References
1	TiO ₂	Hydrothermal, sonochemical, solvothermal, reverse micelles, sol gel, flame spray pyrolysis and nonhydrolytic approach	Optical, electronic, spectral, structural, mechanical and anticorrosion properties	Photocatalysis, dye-sensitized solar cells, gas sensor, nanomedicine, skin care products, waste water treatment by removal of organic and inorganic pollutants and antimicrobial applications	[19–44]
2	ZnO	Sol-gel, homogeneous precipitation, mechanical milling, organometallic synthesis, microwave method, spray pyrolysis, thermal evaporation and mechanochemical synthesis	Optical properties, thermal conductivity, electrical, sensing, transport, magnetic and electronic properties	Electronic and optoelectronic device applications, gas sensor, photocatalytic degradation of organic and inorganic pollutants for waste water treatment, cosmetics, medical filling materials, antimicrobial and anticancerous applications	[45–73]
3	Al ₂ O ₃	Flame spray pyrolysis, reverse microemulsion, sol-gel, precipitation and freeze drying	Optical, transport, mechanical and fracture properties	Waste water and soil treatment by removal of heavy metal ions and antimicrobial applications, ceramic ultrafilters and membranes to remove pathogenic microorganisms, for gas separation, in catalysis and absorption processes and drug delivery etc.	[74–91]
4	SiO ₂	Sol-gel, flame synthesis, water-in-oil microemulsion processes	Physicochemical, optical, luminescent, thermal and mechanical properties	Drug delivery, tissue engineering, carrier for antimicrobial applications, biosensing	[92–100]
5	Magnetic	Co-precipitation, microemulsions, sol-gel techniques, solvothermal, electrochemical, pulsed laser ablation and sonochemical method	Magnetic, calorific, physical and hydrodynamic properties	Biomedicine, cancer treatment, MRI, drug delivery, removal of toxic metal ions and antimicrobial applications	[101–117]
6	Ag	Microwave processing, ultrasonic spray pyrolysis, laser ablation, gamma irradiation, chemical reduction by inorganic and organic reducing agents, photochemical method, thermal decomposition of silver oxalate in water and in ethylene glycol and electrochemical synthesis	Optical properties due to surface plasmon resonance (SPR), antiangiogenic, structural, thermal, electrical and catalytic properties	Antibacterial and antifungal applications in water purification systems, paints and household products, antiviral applications against HIV-I and monkey pox virus, biosensing,	[118–142]
7	Au	Chemical reduction, physical reduction, photochemical reduction, solvent evaporation techniques, microwave irradiation	Optical and photothermal properties due to surface plasmon resonance, thermal, electrical, antiangiogenic, catalytic, magnetic, and thermo-optical properties	Antibacterial and antiviral applications, biosensing, MRI, cancer diagnosis and photothermal cancer therapy	[142–163]

modifiers generates a strong repulsion between nanoparticles. An additional problem found in nanocomposites is a lower impact strength than that found in the organic precursor alone due to the stiffness of the inorganic material, leading to the use of elastomeric additives to increase the toughness of the composites [10]. A polymer-Au nanocomposite was likely the first reported polymer-inorganic nanocomposite (PINC), and it showed interesting optical properties, such as dichroism [11,12]. After the use of Au as an inorganic nano-filler in PINCs for optical applications, the use of other metals including Ag, Pt, Pd, Rh, Cu, and Hg with natural polymers was examined for similar optical applications [12]. The word “nanocomposite” first appeared in a paper from the polymer literature in 1990, describing cars equipped with a polymer-clay

hybrid part driven through towns and fields. Clay-nylon-6 nanocomposites were used to make timing belt covers for a Toyota car, the first commercial example of polymeric nanocomposites in automotive applications [13]. Polymeric nanocomposites have since been used in various applications, such as catalysis, field-responsive materials for electronic and optoelectronic devices, the stationary phase for chromatographic separations, semipermeable heat and fire-resistant hybrid membranes, and films for food packaging and coating.

Furthermore, the joining of biomaterials and semiconductor/metal nanoparticles increases the impact of biophotonics and bioimaging in biological and medical science. The combination of nanotechnology and biology provides the opportunity for the development of new

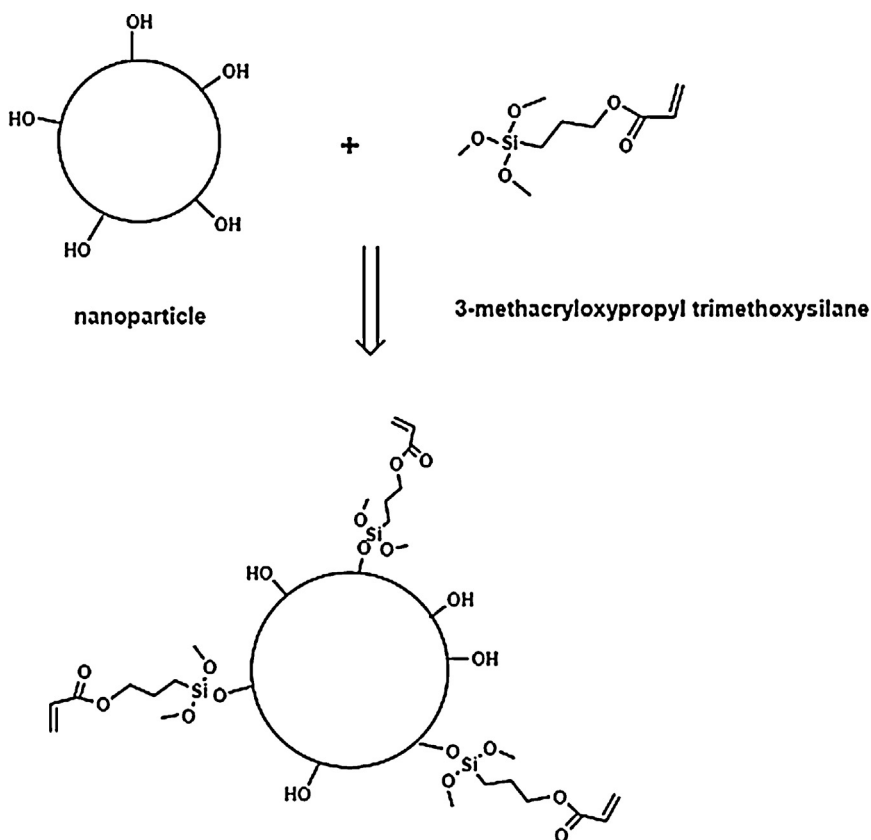


Fig. 1. Modification of a nanoparticle with 3-methacryloxypropyl trimethoxysilane.

Reprinted from [167], Open access 2008.

materials in the nanosize range that can be used in many potential applications in clinical medicine. Unfortunately, typical nanoparticles are eliminated rapidly from the blood stream after being injected because they are recognized by macrophages from the mononuclear phagocyte system [14]. Thus, to increase the circulation time of nanoparticles in the blood stream, it is necessary to modify the particles with polymers such as polyethylene glycol (PEG). Nanoparticles that have been modified with polymers such as PEG are biocompatible, i.e., nonimmunogenic, nonantigenic, and protein resistant [15].

This review is focused on the synthesis and surface modification of inorganic nanoparticles to produce better dispersions in organic solvents or polymer matrices. The methods of synthesis for organic–inorganic nanocomposite materials and various applications of the unmodified and modified nanoparticles and nanocomposite materials are also discussed.

2. Inorganic nanoparticles

2.1. Synthesis, properties and applications of selected inorganic nanoparticles

Nanoparticles may be synthesized from many materials by various physical and chemical methods, with the particles differing in their elemental composition,

shape, size, and chemical or physical properties [16]. The physical methods generally involve vapor deposition and depend on the principle of sub-dividing bulk precursor materials into smaller nanoparticles. The chemical approach generally involves reduction of metal ions into metal atoms in the presence of stabilizing agents, followed by the controlled aggregation of atoms [17]. The synthesis of nanoparticles by chemical methods has proved to be more effective than the use of physical methods.

At nanoscale dimensions, the properties of the material may change significantly to differ completely from their bulk counterparts. As the size of the material decreases, the proportion of surface atoms increases, which increases the reactivity and makes them highly reactive catalysts with the surface atoms the active centers for elementary catalytic processes [18]. Thus, nanoparticles possess unique electronic, optical, magnetic and mechanical properties that arise explicitly due to their nanometer-scale size. Because of these unique properties, NPs can be employed in applications in various fields, such as catalysis, waste water treatment, textiles, paints, drug delivery, magnetic resonance imaging (MRI), tissue engineering, and cancer treatment.

The synthesis, properties, and applications of selected inorganic nanoparticles are summarized in Table 1 [19–163].

3. Surface modification of inorganic nanoparticles

3.1. Chemical treatments

The surface modification of nanoparticles by chemical treatments (such as the absorption of silane coupling agents) is a useful method to improve the dispersion stability of nanoparticles in various liquid media. The concept of silane coupling agents was reported by Plueddemann and his coworkers [164]. After that landmark publication, research proceeded on modified particle surfaces using silane coupling agents to improve the compatibility between the particle and polymer surfaces and the properties of composite materials [165,166]. A nanoparticle modified with a 3-methacryloxypropyl trimethoxysilane coupling agent is shown in Fig. 1. It is seen in Fig. 1, the surface of the unmodified nanoparticle is covered only with –OH groups, while the surface of the silane-modified nanoparticle is covered with 3-methacryloxypropyl trimethoxysilane molecules. The modified nanoparticles behave differently within organic solvents or polymer matrices compared to unmodified nanoparticles, e.g., the modified nanoparticles show comparatively better dispersion in both media [167].

The surface of nanoparticles may also be modified through reactions with metal alkoxides, epoxides, such as propylene oxide, and alkyl or aryl isocyanates [168]. Guo et al. [169] modified silica nanoparticles with 3-(trimethoxysilyl)propyl methacrylate (MPS), a silane coupling agent, and found that the grafting ratio of MPS on the surface of nanosilica increased with MPS content. Kim and White [170] treated nanosilica with silane coupling agents having different aliphatic chain lengths. The surface modification of TiO_2 and ZnO particles has been reported using different silane coupling agents, such as 3-aminopropyltriethoxysilane, n-propyltriethoxysilane and 3-methacryloxypropyltrimethoxysilane [171,172]. Recently, Sabzi et al. [173] carried out surface modification of TiO_2 nanoparticles with aminopropyltrimethoxysilane (APS) and investigated its effect on the properties of a polyurethane composite coating, demonstrating improved mechanical and UV-protective properties of the urethane clear coating. In a more recent study, the dispersion stability of TiO_2 nanoparticles in organic solvents was improved by treating the particle surface with a silane coupling agent [174]. Zhao et al. [175] carried out a surface modification of TiO_2 nanoparticles with the silane coupling agents 3-aminopropyltrimethoxysilane (APTMS) and 3-Isocyanatopropyltrimethoxysilane (IPTMS). The process of nanoparticle surface modification by silane coupling agents is shown in Fig. 2.

Ma et al. [176] improved the dispersion stability of ZnO nanoparticles by treatment with a KH570 silane coupling agent. Shen et al. [177] modified Fe_3O_4 nanoparticles with KH570 silane-coupling agents for better dispersibility in organic solvents. Truong et al. [178] treated the Al_2O_3 nanoparticle surface with two different silane coupling agents, (3-chloropropyl)triethoxysilane and (octyl)triethoxysilane to enhance hydrophobic interactions with the syndiotactic polypropylene matrix. Guo et al. [179] successfully modified alumina

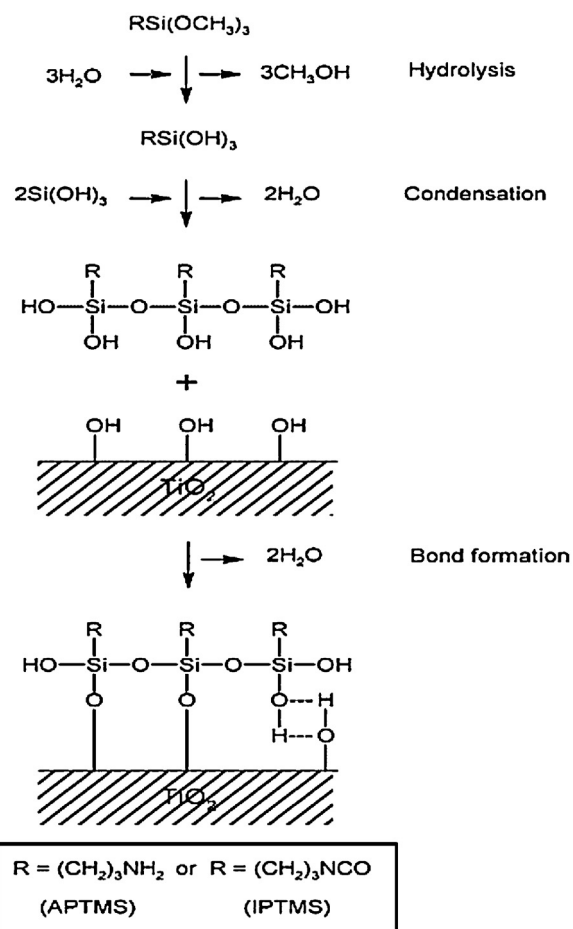


Fig. 2. Chemical grafting of organosilanes onto TiO_2 nanoparticles surface. Reprinted from [175], Copyright 2011, with permission from Elsevier.

nano-particles with a bi-functional coupling agent, (3-methacryloxypropyl)trimethoxysilane, through a facile neutral solvent method. Mallakpour and Barati [180] reported the surface modification of TiO_2 nanoparticles by reaction with a γ -aminopropyltriethoxy silane coupling agent. The silane coupling agent is adsorbed on the surface of the nanoparticles at its hydrophilic end and interacts with hydroxyl groups that are pre-existing on the nanoparticle's surface.

3.2. Grafting of synthetic polymers

Another approach to modify the surfaces of inorganic and organic materials is based on grafting synthetic polymers to the substrate surface, which enhances the chemical functionality and alters the surface topology of the native inorganic and organic materials. Such polymer-grafted inorganic nanoparticles are considered to be organic-inorganic nanocomposite particles.

Because monomers usually have a low molecular weight by their nature, they can penetrate the aggregated nanoparticles and react with the activated sites on the nanoparticle surface. The interstitial volume inside the nanoparticle aggregates becomes partially filled

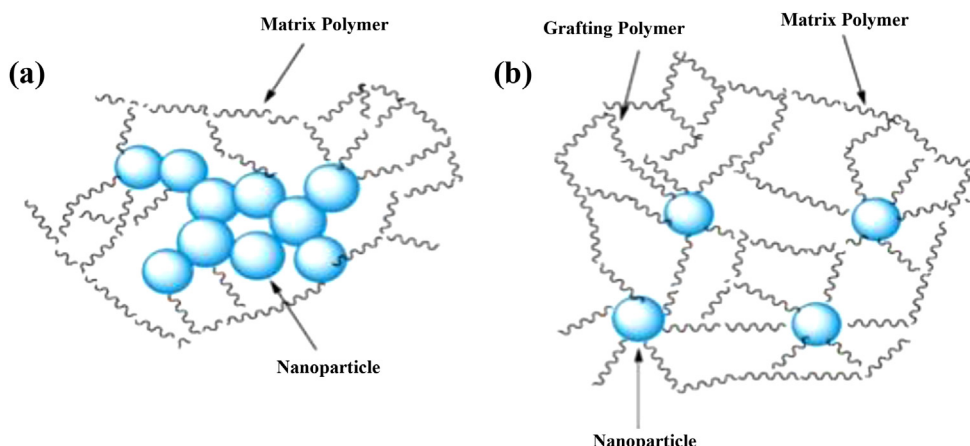


Fig. 3. Schematics of: (a) agglomerated nanoparticles in the matrix polymer in the case without grafting polymer and (b) separation of particles due to the grafting polymer.
Reprinted from [181], Copyright 2001, with permission from Elsevier.

with grafted macromolecular chains, and the aggregated nanoparticles become further separated. In addition, the surfaces of the nanoparticles become hydrophobic, which is important for the miscibility of the filler and matrix. Fig. 3 shows the dispersion behavior of bare and polymer-grafted nanoparticles in a polymer matrix [181].

Two methods have been reported in the literature to covalently graft polymer chains on the surface of inorganic particles. The first method is the “grafting to” method in which the end-functionalized polymers react with an appropriate surface. The second method is the “grafting from” method in which polymer chains are grown from an initiator-terminated self-assembled monolayer [182–184]. The schematic representations of the “grafting to” and “grafting from” methods are shown in Fig. 4 [185].

A higher percentage of successful grafts can be obtained in polymer-grafted inorganic particles by initiating the graft polymerization from initiating groups placed on the particles’ surfaces. The polymerization processes, which may include radical, anionic and cationic polymerization methods, involves propagation of the grafted polymers from the surface of the particle [186]. The method of producing controlled/living radical polymerization from the surfaces of silica nanoparticles using atom-transfer radical polymerization systems was proposed by von Werne and Patten [187]. Rong et al. [188] carried out a surface

modification of nanosized alumina particles by grafting polystyrene and polyacrylamide (PAAM) on the particles. Sidorenko et al. [189] investigated the radical polymerization of styrene and methyl methacrylate (MMA) on the surface of TiO_2 particles by adsorbed hydroperoxide macroinitiators. Wang et al. [190] reported the synthesis of poly(methyl methacrylate)-grafted TiO_2 nanoparticles by a photocatalytic polymerization process. PMMA chains were grafted directly from the surfaces of the TiO_2 nanoparticles in water under sunlight illumination.

Tsubokawa et al. [191] reported on the grafting of hyperbranched polymers having pendant azo groups on silica nanoparticle surfaces, and they subsequently initiated a radical postgraft polymerization of vinyl monomers from the azo groups of those polymer chains. Shirai et al. [192] carried out a radical graft polymerization of vinyl monomers on the surface of polymethylsiloxane-coated titanium dioxide nanoparticles that were further modified with alcoholic hydroxyl groups initiated by the azo groups introduced on Ti/Si-R-OH (Fig. 5 (1)(2)). The graft polymerization of vinyl monomers initiated by a system consisting of trichloroacetyl groups on the titanium dioxide surface interacting with $\text{Mo}(\text{CO})_6$ was also carried out (Fig. 5 (3)).

Fan et al. [193] reported the surface-initiated graft polymerization of methyl methacrylate from TiO_2 nanoparticle

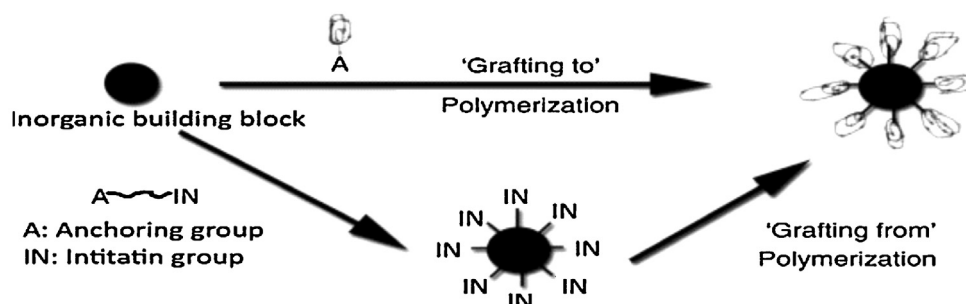


Fig. 4. Schematic description of grafting-to and grafting-from approaches for the synthesis of PINCs.
Reprinted from [185], Copyright 2003, with permission from Elsevier.

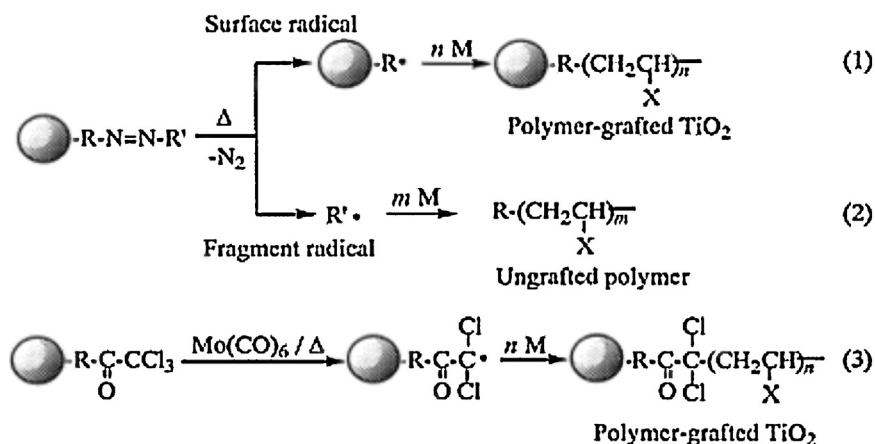


Fig. 5. Radical graft polymerization of vinyl monomers initiated by azo groups introduced onto Ti/Si-R-OH (1)-(2) and by the system consisting of trichloroacetyl groups on titanium dioxide surface and Mo(CO)₆ (3). Reprinted from [192], Copyright 1999, with permission from Elsevier.

surfaces through a biomimetic initiator. Rong et al. [194] reported an irradiation graft polymerization of styrene and methyl methacrylate on magnetic iron, cobalt and nickel nanoparticles under different atmospheres as illustrated in Table 2.

Yokoyama et al. [195] carried out the radical grafting of a biocompatible polymer, 2-methacryloyloxyethyl phosphorylcholine (MPC), on the surfaces of silica nanoparticles, which was initiated either by azo groups previously introduced on the silica surface or by a system consisting of Mo(CO)₆ and trichloroacetyl groups on the silica surface. Tang et al. [196] modified the surface of ZnO nanoparticles by grafting or anchoring polymethacrylic acid chains on the particles' surfaces to create better dispersion in an aqueous system. The -OH groups on a ZnO nanoparticle's surface interact with carboxyl groups (COO⁻) in the PMMA to form a poly(zinc methacrylate) complex on the surface as shown in Fig. 6.

Hong et al. [197] carried out surface modification of ZnO nanoparticles by grafting polymethyl methacrylate (PMMA) on the particles via a free radical polymerization

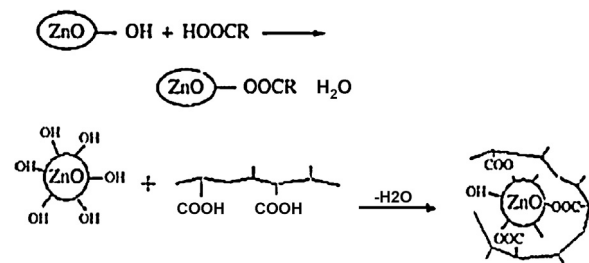


Fig. 6. Reaction scheme for the anchoring or grafting of PMAA on ZnO nanoparticles. Reprinted from [196], Copyright 2006, with permission from Elsevier.

Table 2

Irradiation graft polymerization of methyl methacrylate (MMA) and Styrene (St) onto Fe, Co and Ni nanoparticles under different conditions [Adapted from ref 194, Copyright (2002), with permission from Elsevier].

Monomer/nanoparticles (weight ratio)	Irradiation atmosphere	γ_c^a (%)	γ_e^b (%)	γ_g^c (%)
MMA/Ni (45 nm)=10/1	N ₂	53.7	1.19	5.97
MMA/Ni (45 nm)=10/1	O ₂	78.3	0.75	7.6
St/Ni (45 nm)=10/1	N ₂	69.4	1.62	11.12
St/Ni (45 nm)=10/1	O ₂	42.0	0.51	2.15
MMA ^d /Ni (40 nm)=4/1	N ₂	71.9	8.97	28.13
MMA ^d /Ni (74 um)=1/1	N ₂	78	0	0
MMA ^d /Fe (40 nm)=3/1	N ₂	68.2	1.51	2.75
MMA ^d /Co (33 nm)=3/1	N ₂	79.7	1.36	2.89

Solvent-free, irradiation dose: 10 Mrad.

^a γ_c (monomer conversion): weight of polymer/weight of monomer.

^b γ_e (grafting efficiency): weight of grafted polymer/weights of grafted polymer and homopolymer.

^c γ_g (percent grafting): weight of grafted polymer/weight of nanoparticles.

^d 4 Mrad.

process. In a recent study, Bach et al. [198] grafted PMMA on Fe₃O₄ magnetic nanoparticles (MNPs) by using a "grafting from" approach based on thiol-lactam initiated radical polymerization (TLRP) (Fig. 7).

The graft polymerization of vinyl monomers on silica, titanium dioxide and carbon-black nanoparticles was investigated by Shirai and Tsubokawa [199] using an initiation system consisting of trichloroacetyl groups on the particle surfaces along with molybdenum hexacarbonyl. Liu and Wang [200] reported on the grafting of poly(hydroethyl acrylate) (PHEA) from the surface of ZnO nanoparticles via copper-mediated surface-initiated atom-transfer radical polymerization (SI-ATRP). The surfaces of silica nanoparticles were modified with poly(ethylene glycol) methacrylate (PEGMA) or poly(propylene glycol) methacrylate (PPGMA) for better dispersibility in the polymer matrix. Silica nanoparticles were first treated with triethoxyvinylsilane (VTES) as a coupling agent to allow the introduction of reactive groups, and PEG or PPG molecules were then grafted on the particle surface via UV-photopolymerization. The mechanism to graft PEG or PPG on silica nanoparticles via UV-photopolymerization is presented in Fig. 8 [201].

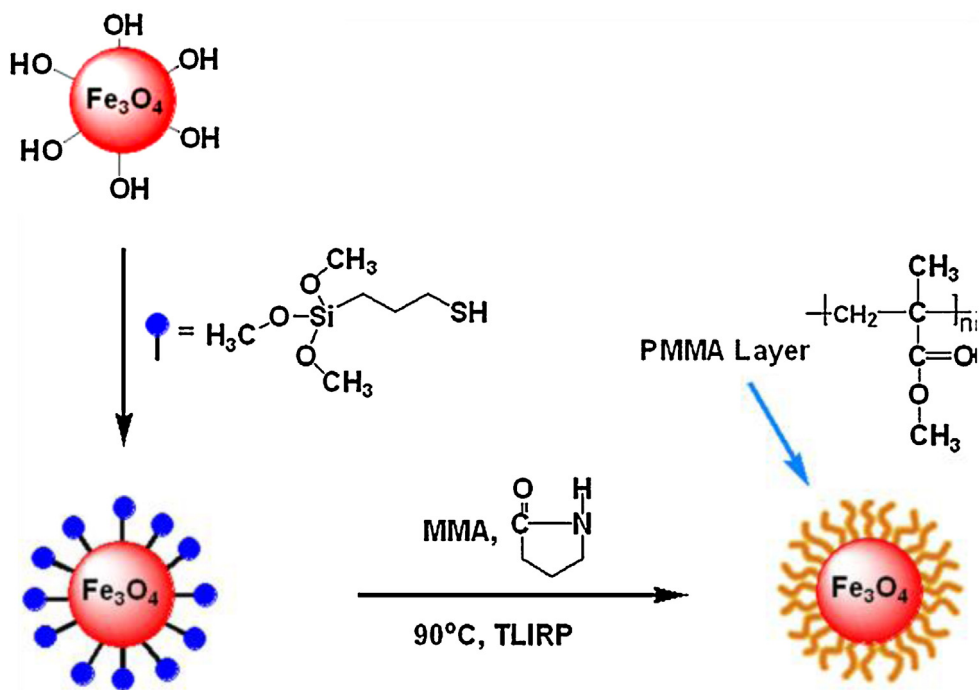


Fig. 7. Synthesis of PMMA-g-MNPs via TLIRP “grafting from” approach.

Reprinted from [198], Copyright 2012, with permission from Elsevier.

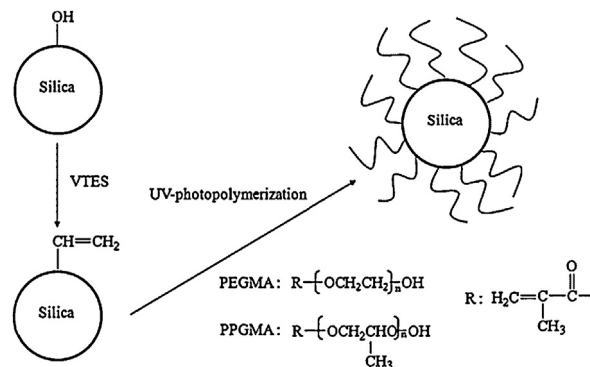


Fig. 8. Mechanism of grafting PEG or PPG onto silica nanoparticles via UV-photopolymerization.

Reprinted from [201], Copyright 2008, with permission from Elsevier.

3.3. Ligand exchange technique

Pioneering work on the synthesis of CdX (X = S, Se, or Te) NPs with a narrow size distribution in molten tri-octylphosphine oxide laid the foundation for the use of classic thermolytic routes, which involves reactions of inorganic precursors with organic solvents at high temperatures [202]. Greenham et al. [203] demonstrated that a few-nanometer-thick ligand layer is enough to shield the NPs and to prevent the transport of free electrons from NP to NP before recombination can occur; thus, this layer significantly hinders charge transfer. Moreover, bulky organic ligands mostly do not have functional end groups that can positively contribute to the charge transport in

a NP-polymer blend. Therefore, it is crucial to remove as many of the synthesis ligands from the NP surface as possible to reduce the distance between NPs and between NP-polymer contacts to avoid recombination losses and enhance charge transport through the photoactive layer. The ideal solution would enhance the transfer of electrons by reducing the separation caused by the organic synthesis ligands surrounding the NPs while maintaining the critical stability of the NP dispersions. This solution can be achieved by exchanging the synthesis ligands with a more suitable ligand. Ideally, the substituted ligand would be removable from the NP surface in the active layer of a solar cell by thermal annealing and/or vacuum processes to enhance the conductivity between the NPs and allow efficient charge separation between the NPs and the polymer.

Many technologically-important, high-quality NPs, such as semiconductor nanocrystals can now be routinely prepared through various modified versions of the thermolytic method. Upon heating the reaction solution to a sufficiently high temperature (typically 150–320 °C), the precursors will be chemically transformed into active atomic or molecular species that can then condense to form NPs. The growth of these NPs is strongly influenced by the presence of capping ligands [204]. The size of the NPs can be controlled by stopping the reaction at different growth stages or by changing the ligand concentrations. NPs with shapes, such as nanodisks, nanorods, and nanoscale polyhedral structures can also be synthesized by taking advantage of the selective adhesion of certain ligands to particular crystalline facets to kinetically control the relative growth rates along different crystalline directions.

Prior studies have demonstrated that the photocurrent in P3HT:CdSe nanorod films increases after thermal annealing, and this effect is ascribed to a decrease in the number of substitution ligands [205]. Nevertheless, the substitution ligands may remain in the film even after annealing; thus, it is preferred that the substitution ligands have at least one π -electron system that could contribute to carrier transport by conjugating to other molecules and surfaces. Finally, the substitution ligands should preferably not form covalent bonds to the semiconducting NPs so that they can easily be removed from the system by annealing. Pyridine, which satisfies the listed criteria, is one of the most widely utilized substitution ligands. The ligand exchange is usually performed by refluxing the CdSe NPs in pyridine; the weakly coordinating but more abundant pyridine replaces the synthesis ligands by mass action. NPs coated with pyridine become insoluble in non-polar aliphatic solvents, but are dispersible in more polar solvents. Alternatively, simple washing methods can also be applied to remove excess ligands surrounding the NPs. Recently, Celik et al. [206] presented an enhanced surface modification method for NPs by combining the advantages of washing methods and ligand exchange, which led to improved solar cell performance with power conversion efficiency (PCE) values approaching 3.5%. They demonstrated the benefits of removing the excess surfactants, which shield the NPs, by adding a washing step prior to ligand exchange. This added step facilitated the replacement of synthesis ligands with pyridine. The removal of surface ligands by various surface treatment methods was analyzed by TGA-MS and the results were compared. An optimized surface modification of NPs improves the charge carrier transport within the photoactive layer and subsequently leads to better photocurrent and device performances.

Zhou et al. [207] reported a synthesis of spherical CdSe quantum dots using hexadecylamine (HDA) as a ligand. The quantum dots are washed with hexanoic acid, which results in salt formation and reduction to a HDA ligand sphere. By applying this method to TOP/oleic acid-capped QDs and HDA-capped QDs, the highest conversion efficiencies for spherical QD hybrid solar cells was achieved with PCE values reaching >2.7%. The post-synthetic surface treatment routes presented so far emphasized either ligand exchange or simple washing methods. Recent approaches to synthesize the inorganic NPs directly in the polymer film during the thermal annealing step are a promising novel approach to overcome the limitations introduced by surface ligands on colloidal NPs [208]. In these approaches, suitable precursor molecules are dissolved in the polymer solution prior to film deposition. The film annealing induces NP formation *in situ* in the polymer film.

Hu et al. [209] reported on a photoassisted ligand exchange approach whereby light was introduced to facilitate the replacement of oleic acid (OA) ligand molecules around PbSe quantum dots (QDs). The ligand-exchanged QDs were used to fabricate quantum dot light-emitting diodes (QD-LEDs), which outperform devices fabricated with QDs without ligand replacement. Earlier work by Lokteva et al. [210] focused on hybrid solar cells prepared from CdSe QDs that were initially capped with oleic acid

(OA), and the impact of single and multiple pyridine treatments was thoroughly investigated. NMR was applied to determine the composition of the ligand shell and to distinguish the bound and free ligands before and after ligand exchange. It was shown that after a single pyridine treatment, some amount of OA was still present in the samples. By using thermal gravimetric analysis (TGA), the authors could also obtain quantitative information about the effectiveness of additional pyridine treatments. In a series of one-, two-, and threefold ligand exchange operations, the estimated surface coverage of OA decreased from 26% to 12%, whereas that of pyridine increased from 54% to 80% [211].

3.4. Other methods of surface modification

Other methods for surface modification of inorganic nanoparticles have been reported, including adsorption of polymeric dispersants and *in situ* surface modification. Surface modification by adsorption of polymeric dispersants is one of the simplest methods to improve the dispersion behavior of nanoparticles in aqueous systems. The hydrophilic nanoparticles can be dispersed in highly polar organic solvents by using anionic or cationic polymer dispersants. These dispersants generate steric repulsive forces among the polymer chains and increase the surface charge, which results in better dispersibility of the nanoparticles. As an example for anionic surfactants, various types of polycarboxylic acids and their salts have been used to disperse many types of oxide nanoparticles, such as TiO₂, Al₂O₃, and Fe₂O₃ [212–214]. Likewise, *in situ* surface modification techniques, which perform surface modification during the nanoparticle synthesis phase, have also been reported in the literature. Examples of these techniques include the reverse micelle method, thermal decomposition of organometallic compounds and polyol methods [215–217]. The capping agents or surfactants, such as tri-octylphosphine oxides (TOPO), oleic acid and amines, are dissolved in the synthesis solution to prevent the agglomeration of nanoparticles. Surfactant-capped nanoparticles that have been synthesized by the *in situ* surface modification method can be further modified to tune their surface properties.

4. Applications of modified inorganic nanoparticles

4.1. Dispersion of surface modified nanoparticles in organic solvents

The dispersion stability of ultrafine inorganic particles in organic solvents or polymer matrices is known to be remarkably improved when polymers have been grafted on their surfaces. The polymer chains grafted on the surface of nanoparticles prevent aggregation of the particles and increase the affinity of the surface for the solvent or polymer matrix. For example, the dispersion stability of polyMMA-grafted titanium dioxide in THF was compared with that of Ti/Si-R-OH. The polymer-grafted titanium dioxide obtained by graft polymerization existed in a stable colloidal dispersion in the THF. Conversely,

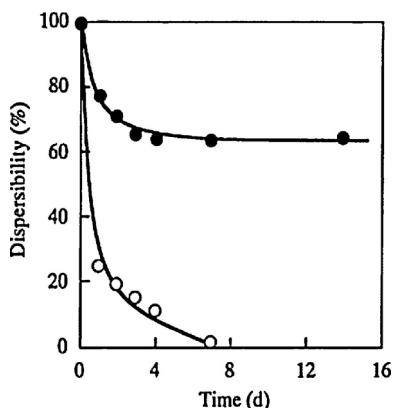


Fig. 9. Stability of MMA-grafted TiO_2 dispersion in THF at room temperature. (●) MMA-grafted (grafting 347.4%); (○) untreated $\text{Ti}/\text{Si}-\text{R-OH}$. Reprinted from [192], Copyright (1999), with permission from Elsevier.

the $\text{Ti}/\text{Si}-\text{R-OH}$ particles undergo complete agglomeration within one week as shown in Fig. 9 [192].

Hong et al. [218] performed a sedimentation test to examine the effect of surface modification on the dispersion behavior of ZnO nanoparticles, and they showed that bare ZnO nanoparticles completely precipitated after 4 h while polystyrene-grafted ZnO nanoparticles formed a stable dispersion in acetone (Fig. 10). The TEM images shown in Fig. 11 also supported the same result.

Kobayashi et al. [219] studied the dispersion stability of bare and grafted metal-oxide nanoparticles. Using TEM images (Fig. 12), the study revealed that ungrafted Fe_3O_4 and TiO_2 nanoparticles formed aggregates of several hundred nanometers in diameter. In comparison, PS-grafted Fe_3O_4 and TiO_2 nanoparticles were finely dispersed in groups of one or two particles. Rong et al. [188] compared the dispersibility of polymer-grafted alumina in a solvent (Al_2O_3 -g-PS in THF and Al_2O_3 -g-PAAM in acetone) with untreated alumina (Fig. 13). The results showed a remarkable improvement in the dispersibility resulting from the surface grafting procedure; untreated alumina completely precipitated after a few hours.

Tang et al. [220] compared the dispersion stability of poly(MMA-MAA)-grafted ZnO nanoparticles in toluene

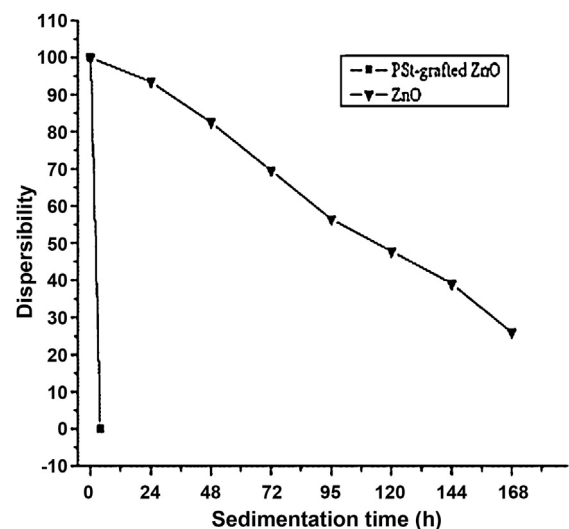


Fig. 10. Sedimentation of bare and PSt-grafted ZnO nanoparticles in acetone. Reprinted from [218], Copyright 2009, with permission from Elsevier.

with that of bare ZnO nanoparticles. They observed that the bare nanoparticles precipitated completely within one day whereas the poly(MMA-MAA)-grafted ZnO nanoparticles created a stable colloidal dispersion in toluene. These results indicate that a stable dispersion of grafted nanomaterials occurs due to the steric repulsion among polymer chains, which arises from the osmotic pressure, and the affinity of surface polymer chains for itself rather than the solvent. These reports demonstrate that polymers grafted on the nanoparticle surfaces can strongly influence the dispersion behavior of nanoparticles in various solvents. The silane-functionalized nanoparticles also show better dispersibility in organic solvents or polymer matrices. For example, the dispersibility of silane-functionalized alumina nanoparticles in syndiotactic polypropylene (Spp) has been investigated. The silane-modified alumina nanoparticles showed good dispersibility in the polymer matrix [178]. The dispersion stability of ZnO , TiO_2 and Fe_3O_4 nanoparticles was also improved after surface modification with silane coupling agents [174,176,177].

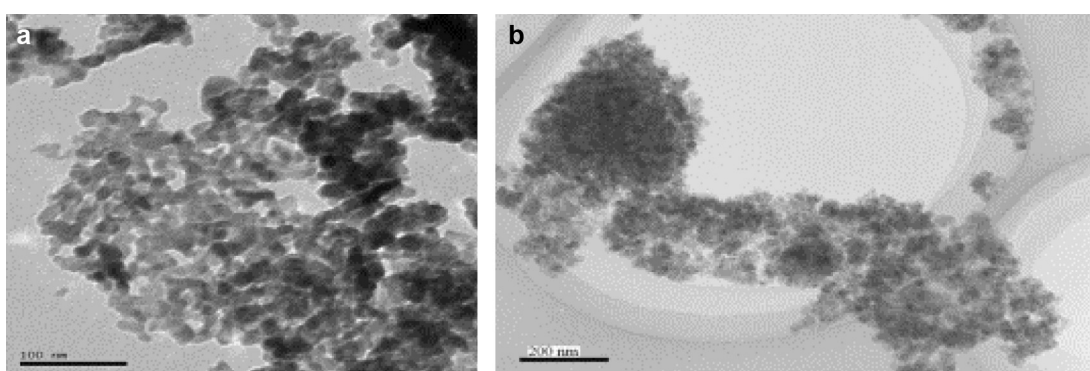


Fig. 11. TEM photographs of: (a) bare ZnO nanoparticles; (b) PSt-grafted ZnO nanoparticles. Reprinted from [218], Copyright 2009, with permission from Elsevier.

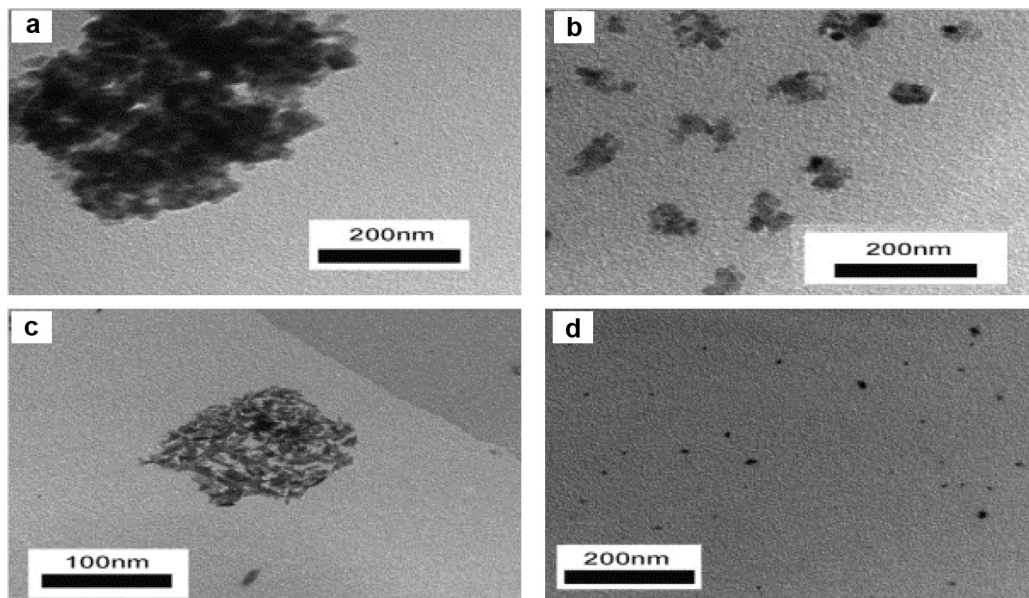


Fig. 12. TEM images of non-grafted Fe₃O₄ ($d \approx 10$ nm) particles (a), PS-grafted Fe₃O₄ (b), non-grafted TiO₂ ($d \approx 10$ nm) particles (c), and PS-grafted TiO₂ dispersed in chloroform (0.01 mg/mL) (d).
Reprinted from [219], Copyright 2006, with permission from Elsevier.

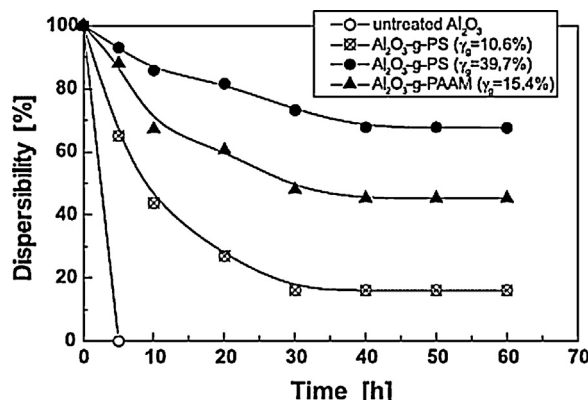


Fig. 13. Dispersibility of Al₂O₃-g-PS in THF and Al₂O₃-g-PAAM in acetone at room temperature.
Reprinted from [188], Copyright 2002, with permission from Elsevier.

4.2. Photocatalytic and antibacterial applications

Because of their photocatalytic and antibacterial properties, semiconductor nanoparticles (for example, ZnO and TiO₂) find applications in food packaging, self-cleaning and antifouling materials, and water purification membranes. Tristantini et al. [221] modified TiO₂ nanoparticles with PEG and SiO₂ to promote antifogging and self-cleaning applications. Polypyrrole- [222], polythiophene- [223] and polyaniline- (PANI) [224] modified TiO₂ have been investigated, and they showed photocatalytic activity that promotes degradation of methyl orange and phenol. Song et al. [225] modified the TiO₂ nanoparticles by adding poly(fluorine-co-bithiophene) to promote photocatalytic degradation of organic pollutants, such as phenol under

visible light irradiation. Furthermore, surface modification is necessary to allow the use of these nanoparticles in cosmetics, such as in sunscreens, in an effort to reduce the production of OH[·] free radicals. Hong et al. [218] carried out surface modification of ZnO nanoparticles by grafting polystyrene to improve their dispersibility, to reduce photocatalytic properties, and to obtain good UV-shielding capability to promote their use in cosmetics. Ukaji et al. [171] investigated the effect of surface modification of TiO₂ particles with 3-aminopropyltriethoxysilane (APTES) and n-propyltriethoxysilane (PTES) on the particles' photocatalytic activity and UV-shielding ability. The fine TiO₂ particles modified with APTES showed lower photocatalytic activity and greater UV-shielding ability in comparison with the PTES modified particles. Zhao et al. [175] studied the photocatalytic properties of silane-modified TiO₂ nanoparticles and observed that an increase in the organosilane ratio from 0 wt.% to 200 wt.% caused the rate constant for 3-aminopropyltrimethoxysilane - TiO₂ photocatalytic activity to decrease slightly and for 3-isocyanatopropyltrimethoxysilane-TiO₂ to decrease rapidly, and the effect was significantly dependent upon the grafting efficiency. Inbaraj et al. [226] studied the antibacterial properties of superparamagnetic nanoparticles modified with glycol chitosan (GC) against *Escherichia coli* ATCC 8739 and *Salmonella enteritidis*. The results obtained from an agar dilution assay showed that both bare and GC-modified nanoparticles inhibited the growth of both bacteria types better than the antibiotics linezolid and cefaclor. Galindo et al. [227] modified the surface of ZnO nanoparticles by using 3-aminopropyltrimethoxysilane and di-functional alcohol spiroorthocarbonate to use ZnO nanoparticles in significant antimicrobial medical devices.

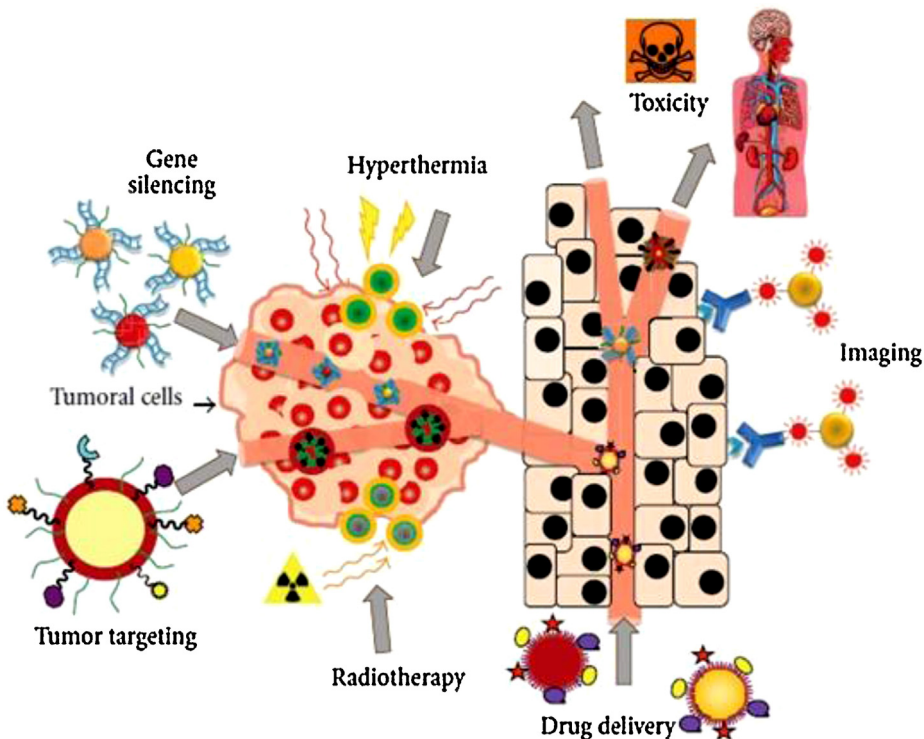


Fig. 14. Various biomedical applications of metal nanoparticles for cancer therapy.

Reprinted from [228], Open access 2012.

4.3. Biomedical applications of surface modified nanoparticles

Inorganic nanoparticles, especially noble metal nanoparticles, have a wide range of biomedical applications in biosensing, as contrast agents in magnetic resonance imaging (MRI), for tissue engineering, in tumor destruction by heating (hyperthermia), and for targeted drug and gene delivery. Various biomedical applications of metal nanoparticles are shown in Fig. 14 [228]. In these applications, the nanoparticles are usually functionalized either with various sensing agents, such as antibodies, peptides, DNA and RNA to target specific cells [229] or with biocompatible polymers, such as PEG to increase their *in vivo* circulation time for drug and gene delivery applications [230].

The biocompatibility of nanoparticles can also be enhanced by conjugation or through the incorporation of ligands on their surface, such as targeting agents, permeation enhancers, optical dyes, and therapeutic agents. For example, the structure of biocompatible magnetic nanoparticles with multifunctional groups is shown in Fig. 15 [231].

Zhang et al. [230] carried out surface modifications of superparamagnetic nanoparticles with PEG and folic acid to improve their intracellular uptake and ability to target specific cells, respectively. Cheyne et al. [232] reported the synthesis of biocompatible TiO₂ nanoparticles containing a functional NH₂ or SH group. These nanoparticles could be functionalized with organic moieties for

use in biomedical applications, such as medical imaging and radioimmunotherapy where ultrasmall nanoparticles are essential for rapid renal clearance. Kohler et al. [233,234] reported the development of a methotrexate (MTX) immobilized iron-oxide nanoparticle drug carrier for sustained delivery of MTX in breast and brain tumor cells. The MTX was covalently attached to amine-functionalized iron-oxide nanoparticles through the amide bonds to ensure stability of the drug conjugate under intravenous conditions. Chertok et al. [235] investigated the use of polyethylenimine-modified magnetic iron-oxide nanoparticles for the delivery of drugs and genes to brain tumors. Shen et al. [236] and Josephson et al.

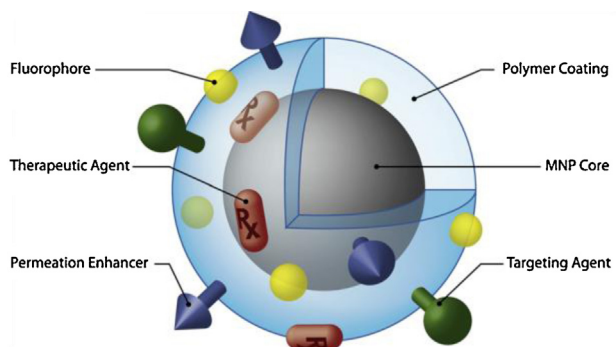


Fig. 15. Magnetic nanoparticles possessing various ligands to enable multifunctionality from a single nanoparticle platform.
Reprinted from [231], Copyright 2008, with permission from Elsevier.

[237] reported various formulations of dextran-coated iron-oxide nanoparticles, also known as monocrystalline iron-oxide nanoparticles (MION), and crosslinked iron-oxide nanoparticles (CLIO), which are intended for use in a variety of MR imaging applications. The chemical functionality of CLIO nanoparticles can be established by treating them with ammonia to provide primary amino groups for the subsequent attachment of biomolecules, such as proteins or peptides [238,239]. These nanoparticles have proven to be very effective for drug delivery applications, for example, for the delivery of anticancer drugs. They have significant advantages, such as the ability to target specific locations in the body and to reduce the overall amount of drug used, and they can potentially reduce drug concentrations at non-target sites, which results in fewer side effects.

4.4. Removal of heavy metal ions

Toxic organic or inorganic pollutants, such as alkylphenols and heavy metal ions, are hazardous to public health due to their high toxicity. The major source of metallic pollutants in aquatic systems is the discharge of untreated industrial effluents from industries, such as electroplating, dyeing, battery manufacture, mining operations, chemical manufacture, tanneries, glass manufacture, and pharmaceuticals. The presence of metals, such as chromium, cadmium, arsenic, zinc, lead and mercury in bodies of water is becoming a severe environmental and public health problem. This problem could be overcome by removal of the contaminants via a sorption process. Investigations by many researchers have discovered that the sorption efficiency of porous inorganic materials, such as clays [240,241] and nanoporous and mesoporous silica [242,243], could be improved by grafting organic groups on these inorganic materials. These organic functional groups are grafted on the inorganic materials by stable covalent bonding, and the product shows strong affinities to certain classes of toxic contaminants. Therefore, the grafted sorbents can capture the toxic contaminants selectively even if their concentration is extremely low. Takafuji et al. [244] reported the synthesis of poly(1-vinylimidazole)-grafted magnetic nanoparticles and described their application in the removal of heavy metal ions. The order of removal efficiency for metal ions by these particles was found to be $\text{Cu}^{2+} > \text{Ni}^{2+} > \text{Co}^{2+}$ as shown in Fig. 16.

Pu et al. [245] modified nano-alumina particles with γ -mercaptopropyltrimethoxysilane and used the modified alumina as a solid-phase adsorption material for trace amounts of Hg, Cu, Au and Pd as determined by inductively-coupled plasma mass spectrometry (ICP-MS). The adsorption capacity of modified nano-alumina was found to be 10.4, 16.3, 15.3, and 17.4 mg g⁻¹ for Hg, Cu, Au and Pd, respectively, under optimized conditions.

Yang et al. [246] described that thiol-grafted Al_2O_3 nanofibers can efficiently remove Pb^{2+} and Cd^{2+} ions from water. The pure $\gamma\text{-Al}_2\text{O}_3$ nanofibers FA(S) can remove 40% of Pb^{2+} ions in solution, and the sorption rate of Pb^{2+} ions does not change substantially with variations in the flux.

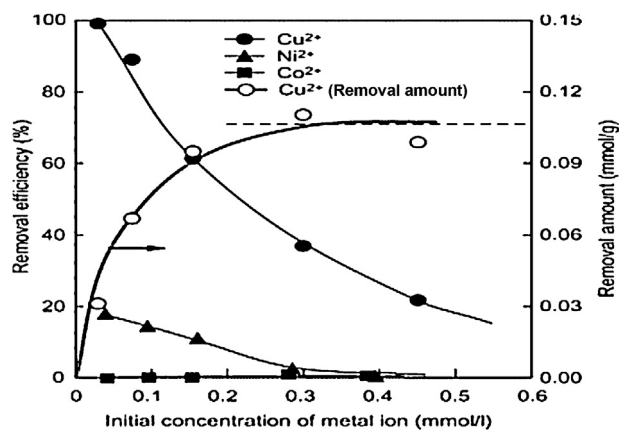
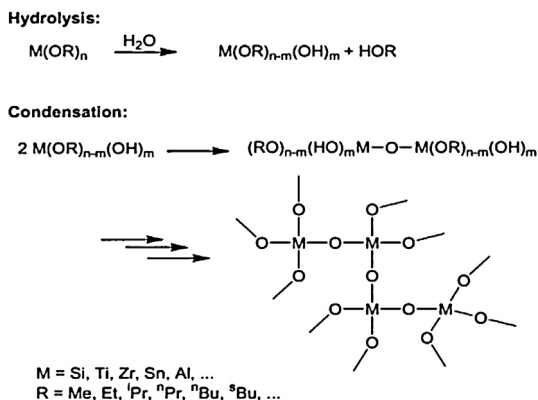


Fig. 16. Removal efficiency of Cu^{2+} , Ni^{2+} , and Co^{2+} and loading capacity of on Mag-Im18 for Cu^{2+} . Metal ion solution/Mag-Im18 10 mL/10 mg. Initial pH of solution = 5.3. Reprinted from [244]. Copyright 2004, with permission from American Chemical Society.

The grafted nanofibers also displayed much higher sorption abilities: SH-FA(S)-1 can remove 60, 67, and 74% of the Pb^{2+} ion sorption at fluxes of 10, 5, and 3 mL/min, respectively. On the other hand, SH-FA(S)-2 shows comparatively better abilities because it was shown to remove 82, 90, and 95% of the ions at the three flux rates, respectively, which are more than twice the sorption ability of the parent bare fibers. Similar results were also reported for the removal of Cd^{2+} ions. Recently, Pang et al. [247] developed a polyethylenimine-grafted porous magnetic adsorbent for highly effective adsorption of heavy metals. Their results showed that the adsorption rates of Cu^{2+} , Zn^{2+} and Cd^{2+} were dependent on pH with increases in pH improving the removal of metal ions. The sorption isotherms of the adsorbent for these metals were well-fitted by a Langmuir model with maximum adsorption capacities of 157.8, 138.8 and 105.2 mg/g for Cu^{2+} , Zn^{2+} and Cd^{2+} , respectively.

5. Organic–inorganic nanocomposite materials

Over the past two decades, scientists have shown significant scientific and technological interest in polymer–inorganic nanocomposites (PINCs). The incorporation of inorganic nanoparticles into polymer matrices can result in novel high-performance materials that find applications in many industrial fields. Various types of inorganic particles have been used in polymer/inorganic particle nanocomposites including metals (e.g., Al, Fe, Au, and Ag), metal oxides (e.g., ZnO , Al_2O_3 , CaCO_3 , and TiO_2), non-metal oxides (e.g., SiO_2) and others (e.g., SiC). Selection of the correct nanoparticle depends on the desired thermal, mechanical, and electrical properties of the resulting nanocomposites. For example, Al_2O_3 nanoparticles can be used for their high conductivity; calcium carbonate (CaCO_3) particles are selected because of their low cost; and silicon carbide (SiC) nanoparticles are used because of their strength, hardness and corrosion resistance [248].

**Fig. 17.** Sol-gel Process.

Reprinted from [249], Copyright (1990, with permission from Academic Press Toronto.

5.1. Methods of synthesis

5.1.1. Sol-gel processing

The sol-gel processing of nanoparticles inside of a polymer dissolved in non-aqueous or aqueous solutions results in the formation of interpenetrating networks between inorganic and organic moieties at mild temperatures; this network improves the compatibility between constituents and builds strong interfacial interaction between the two phases as described in Fig. 17. This process has been used successfully to prepare nanocomposites with silica, alumina, calcium oxide, and titania in a wide range of polymer matrices [249].

Several sol-gel process strategies can be applied to form hybrid materials. One method involves the polymerization of organic functional groups from a preformed sol-gel network; vinyl or epoxy groups and free radical or cationic polymerization processes are common [250,251]. Hsieh et al. [250] reported the synthesis of PS/silica nanocomposites by a sol-gel method. The miscibility of the PS-silica copolymers was enhanced by covalent incorporation of silica into a PS matrix. Alternatively, sol-gel hydrolysis and condensation of a precursor, such as tetraethyloxysilane (TEOS), tetrabutyl titanate, or aluminum iso-propoxide can be carried out starting from a preformed functional organic polymer, such as polyvinyl acetate, polymethylmethacrylate [252], polyetherimide [253], polyvinyl alcohol [254], polyamides [255], polyimide (PI) and several other polymers [256]. Wu [257] reported the synthesis of novel PCL/TiO₂ and PCL-g-AA/TiO₂ nanocomposites by using tetra isopropyl ortho titanate (TTIP) and polycaprolactone (PCL) as the ceramic precursor and the continuous phase, respectively, via an in situ sol-gel process. Du et al. [258] carried out the sol-gel synthesis of a ZnO/polyvinylpyrrolidone nanocomposite thin film for superoxide radical sensor applications. Hu and Marand [259] reported the in situ synthesis of nano-sized TiO₂ domains within poly(amide-imide) by a sol-gel process. The composite films obtained exhibit excellent optical transparency. Garcia et al. [260] carried out the synthesis of nylon-6/SiO₂ nanocomposites by a sol-gel method.

5.1.2. In situ polymerization

In situ polymerization is a method in which inorganic nanoparticles are first dispersed in a monomer, and the resulting mixture is polymerized using a technique similar to bulk polymerization. Ou et al. [261,262] reported the synthesis of nylon-6/silica and nylon-6/potassium titanate nanocomposites by an in situ polymerization method. Guan et al. [263] carried out the synthesis of transparent polymer nanocomposites containing ZnS nanoparticles using a one-pot route via an in situ bulk polymerization process. Jiang [264] reported the synthesis of magnetic nanocomposites containing Ni_{0.5}ZnO_{0.5}Fe₂O₄ nanoparticles via a wet chemical method that leads to a colloidal suspension, which is followed by in situ polymerization of the monomers. Cheng et al. [265] synthesized ZnS-containing transparent polymer nanocomposites by an in situ bulk polymerization method. PMMA/TiO₂ nanocomposites were synthesized by an in situ radical polymerization of MMA in a toluene solution of surface-modified TiO₂ nanoparticles [266]. Yari and Sedaghat [267] carried out the synthesis of platinum-polyaniline nanocomposites by in situ oxidative polymerization of aniline and reduction of Pt⁺⁴ ions into Pt nanoparticles. Park et al. [268] used an in situ polymerization method to synthesize iron oxide-epoxy vinyl ester nanocomposites. Evora and Shukla [269] carried out the synthesis of polyester/TiO₂ nanocomposites by in situ polymerization. The in situ polymerization method was also used for the synthesis of poly(methyl methacrylate)/palladium nanocomposites [270]. Chaichana et al. [271] described the effect of nano-SiO₂ particle size on the formation of LLDPE/SiO₂ nanocomposites synthesized via an in situ polymerization with a metallocene catalyst.

5.1.3. Blending

The most conventional and simple method for the synthesis of polymer/inorganic nanocomposites is direct mixing of the nanoparticles into the polymer. The mixing can generally be done by melt blending or solution blending. The main difficulty in the mixing process is achieving an effective dispersion of the nanoparticles in the polymer matrix because they have a strong tendency to form agglomerates.

5.1.3.1. Solution blending. Solution blending is a liquid-state powder processing method that provides a good level of molecular mixing and is widely used in material preparation and processing. Some of the limitations of melt mixing (described below) can be overcome if both the polymer and the nanoparticles are dissolved or dispersed in solution, but there is a cost depending on the solvent and its recovery [272]. In a study, van Zyl et al. [273] used solution blending to synthesize PA/silica nanocomposites. They dissolved nylon-6 in formic acid while controlling the pH of the solution and then added a solution of silica with particle sizes in the range of 10–30 nm under continuous stirring at room temperature. The solution was then cast, and the solvent was evaporated. Li et al. [274] synthesized polyurethane-based networks filled with ZnO nanoparticles (diameter ~27 nm) via solution blending. They also fabricated ZnO/PU films and coatings from solution by a

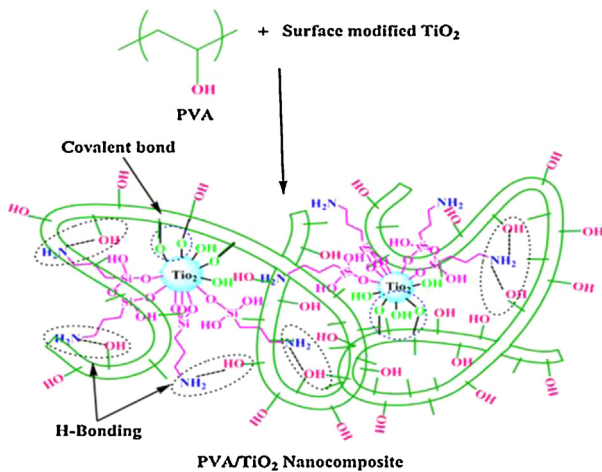


Fig. 18. Schematic illustrations for the preparation of PVA/TiO₂ nanocomposite.
Reprinted from [180], Copyright 2011, with permission from Elsevier.

simple casting and evaporation method. Wang and Kim [275] carried out the synthesis of nanocomposite polymer electrolytes composed of poly(vinylidene fluoride), lithium perchlorate (LiClO₄) and TiO₂ via a solution-casting technique. Recently, poly(vinyl alcohol)/titanium dioxide (PVA/TiO₂) nanocomposite coatings have been synthesized with different loadings of modified TiO₂ with an ultrasonic irradiation process; these nanocomposite coatings were used to synthesize PVA/TiO₂ films via a solution-casting method as shown in Fig. 18 [180].

5.1.3.2. Emulsion or suspension blending. Emulsion blending, also known as suspension blending, is quite similar to solution blending; the only difference lies in the use of an emulsion or suspension solution instead of a simple solution. This method is effective in cases where polymers are difficult to dissolve. Superparamagnetic magnetite/polystyrene composite particles were synthesized by inverse-emulsion polymerization with a water-based magnetic fluid acting as the dispersing phase and organic solvent and styrene acting as the continuous phase [276]. Zhang et al. [277] carried out the synthesis of SiO₂/polystyrene nanocomposite particles of different morphologies by a mini-emulsion polymerization technique. Wang et al. [278] synthesized a nanosilica/polyacrylate organic–inorganic composite emulsion by in situ emulsion polymerization of methyl methacrylate (MMA) and butyl acrylate (BA) in the presence of silane-modified silica nanoparticles. Caris et al. [279] encapsulated the TiO₂ nanoparticles in poly(methyl methacrylate) with a conventional emulsion polymerization. Erdem et al. [280] encapsulated TiO₂ nanoparticles by mini-emulsion polymerization of styrene where polybutene-succinimide pentamine was used as the stabilizer at the oil/water interface.

5.1.3.3. Melt blending. In melt processing, particles are dispersed into a polymer melt and polymer inorganic nanocomposites are then obtained by extrusion. Polypropylene/silica nanocomposite filaments have been

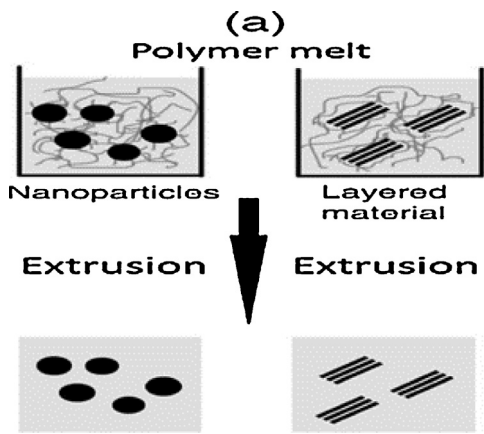


Fig. 19. Melt compounding for preparation of nanocomposites.
Reprinted from [284], Open access 2010.

prepared by direct mixing of components followed by melt compounding using a twin-screw extruder prior to spinning [281]. Surface-treated ZnO nanoparticles were also dispersed in polypropylene via extrusion [282]. Kim et al. [283] carried out the synthesis of PEN composites filled with silica nanoparticles by melt blending to improve the mechanical and rheological properties of PEN. Fig. 19 gives an overview of the melt blending method [284].

Rong et al. [7] carried out the processing of PP/silica nanocomposites in a twin-screw extruder by melt blending. Hong et al. [285] reported that nano-ZnO and low-density polyethylene were melt compounded in a high-shear mixer to prepare nanocomposites with an increased resistance to thermal degradation. Ma et al. [286] reported the synthesis of polystyrene resin/ZnO nanocomposites by melt blending. Chan et al. [287] reported the synthesis of polypropylene/CaCO₃ nanocomposites by melt mixing, and conducted J-integral tests that showed a dramatic 500% increase in fracture toughness. Bhimaraj et al. [288] synthesized a nanocomposite by melt mixing polyethylene terephthalate (PET) with nanoalumina under an inert atmosphere in a batch melt mixer; the wear resistance of PET increased to nearly twice its unmodified value with the addition of 2 wt% 38 nm diameter alumina particles.

5.1.4. *In situ* growth of nanoparticles in a polymer matrix

One simple and efficient method to incorporate inorganic NPs into polymer composites consists of performing *in situ* growth inside the polymer matrix [289–292]. In this method, the particles are generated from their respective particle precursors in the presence of the polymer matrix. The incorporation of precursors into the polymeric matrix is usually achieved either from the gas or liquid phases, but it is possible, though unusual, to mix the components in the solid phase. This step is followed by the removal of undesired (unbound) chemical products after the NPs have formed. Various pathways including chemical reductions, photoreductions, and thermal decompositions can be used for the *in situ* fabrication of NPs [293,294]. Eisa et al. [295] used a simple, cost-effective and environmentally-friendly method for the *in situ* fabrication of Ag NPs in

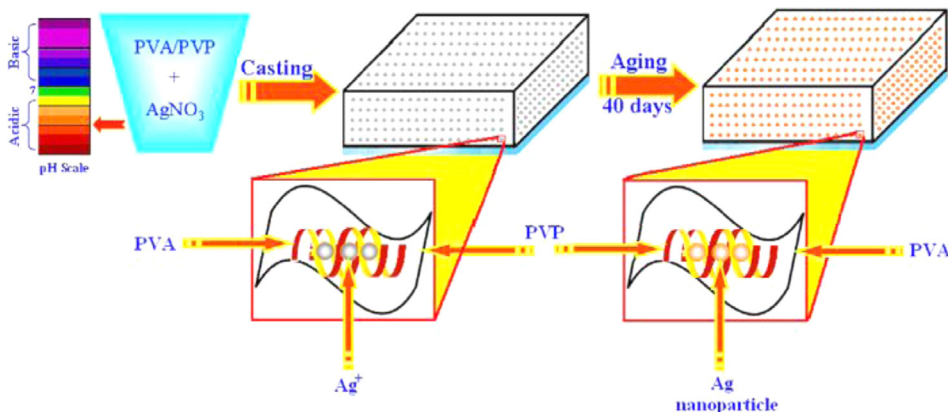


Fig. 20. In situ growth of Ag nanoparticles in PVA/PVP films.

Reprinted from [295], Copyright 2012, with permission from Elsevier.

polyvinyl alcohol (PVA)/polyvinyl pyrrolidone (PVP) films as depicted in Fig. 20. In this method, silver nitrate was reduced to silver, which nucleated and grew within the polymer matrix. A surprisingly excellent integration of Ag NPs into the polymer matrix was achieved without any surface modification of the Ag NPs. Polymer nanocomposites consisting of polyphenylene sulphide and CdS were synthesized by in situ growth of CdS using different cadmium salts, such as cadmium nitrate, cadmium chloride and cadmium acetate. It was reported that only cadmium nitrate yielded CdS NPs, and they had an average size of 15 nm [296]. Suh et al. [297] reported a versatile and cost effective approach to create non-spherical magnetic microparticles via stop-flow lithography and in situ growth of magnetic NPs inside polymer particles. They performed the homogeneous functionalization of the polymeric microparticles with carboxyl groups using stop-flow lithography, and then in situ co-precipitation was used for the growth of MNPs at the carboxyl sites.

Nanocomposites consisting of PVA with Ag and Au NPs were synthesized by in situ growth of Ag and Au NPs inside the polymer matrix with the polymer acting as both the reducing agent and the stabilizer [298].

In situ fabrication of NPs in a polymer matrix has been shown to improve interfacial interactions, including those that are electronic-driven, between NPs and the polymer matrix. For example, cadmium telluride (CdTe) nanocrystals were synthesized in a poly(3-hexylthiophene) (P3HT) matrix without the use of any surfactants, and spectroscopy studies suggest that the nanocrystals are bound to the P3HT via dipole-dipole interactions and form a charge transfer complex [299]. To avoid the aggregation of inorganic NPs in the polymer matrix, Zhou et al. [300] carried-out in situ growth of dicalcium phosphate dehydrate nanocrystals in a biodegradable polymer matrix, i.e., polylactide, using a calcium hybrid as the calcium source.

Another approach consists of the simultaneous formation of both the polymeric matrix and the NPs, and it is considered to be a promising methodology for the synthesis of inorganic-polymer nanocomposites. In this approach, precursors of the NPs are dispersed into polymerisable monomers, and the polymer matrix is created simultaneously during the generation of the NPs. Hence, the in situ

metal surfaces that are formed can catalyze or initiate the polymerization through a transfer of electrons from the metal surface atoms to the monomers. Thus, the degree of dispersion of the inorganic components may affect the formation of the NPs, which affects in turn the degree of polymerization achieved by the polymeric matrix and its rate. Some vinyl monomers have been polymerized in the presence of mechanically dispersed inorganic compounds including some metals (Fe, Al, Mg, Cr, and W). Organometallic compounds have also been used as metal precursors to synthesize nanoparticles in the presence of monomers capable of forming polymer matrices. For example, MMA was polymerized in the presence of bis-triethylgermylcadmium, which decomposes at temperatures close to the polymerization temperature. Similarly, sols of Rh, Pd, Pt, Ag and Au were obtained in PMMA by in situ polymerization of MMA [301]. Polymerization of MMA initiated by AIBN in the presence of silver trifluoroacetate with sequential post-heating resulted in the formation of a Ag/PMMA nanocomposite with an average Ag particle diameter of 310 nm [302]. Au and Pd were incorporated in PAAM-based nanocomposites via an ultraviolet irradiation technique at room temperature. This technique leads to the simultaneous formation of colloidal metal particles by photo-reduction and acrylamide (AM) monomer matrix by photo-polymerization [303]. Silver/PANI nanocomposites were prepared via in situ reduction of silver salt in aniline by mild photolysis at two wavelengths: 365 and 254 nm. The reduction of silver salt in aqueous aniline leads to the formation of silver NPs that, in turn, catalyze the oxidation of aniline to PANI [304]. By changing the synthesis pathway, Tamboli et al. [305] obtained nanowires made of Ag/PANI nanocomposite with diameters ranging from 50–70 nm. In this method, ammonium persulfate was used as an oxidizing agent in the presence of dodecylbenzene sulfonic acid (DBSA) and silver nitrate (AgNO_3).

5.2. Properties of organic-inorganic nanocomposites

5.2.1. Mechanical properties

The main reason to incorporate inorganic particles into polymer matrices is to produce a product with improved mechanical properties (including tensile strength,

flexural strength, hardness, Young's modulus or stiffness) via reinforcement mechanisms as described in theories of nanocomposite materials [306–308]. Ou et al. [261] studied the mechanical properties of nylon-6 reinforced with silica nanoparticles and observed that a loading of 5 wt% silica nanoparticles (50 nm) in nylon-6 increases the tensile strength by 15%, the strain-to-failure by 150%, the Young's modulus by 23% and the impact strength by 78%. The mechanical properties of ABS (acrylonitrile butadiene styrene) filled with both microsized and nano-sized calcium carbonate particles has been investigated [309]. The results showed that the ABS/micron-sized particle composites had a higher Young's modulus but lower tensile and impact strengths than pure ABS whereas the ABS/nanoparticle composites increased the Young's modulus and impact strength. The fracture toughness of nominally-brittle polyester resin systems was improved by incorporating Al_2O_3 nanoparticles [310]. Wang et al. [311] studied the tribological and electrochemical corrosion behaviors of Al_2O_3 /polymer nanocomposite coatings by using micro-hardness tests, single-pass scratch tests, abrasive wear tests, and finally electrochemical techniques, such as potentiodynamic polarization measurements. The addition of Al_2O_3 nanoparticles improved the scratch and abrasion resistance of the polymer coating.

Fig. 21 shows the variation in quasi-static fracture toughness as a function of the volume percentage of TiO_2 in a polyester/ TiO_2 nanocomposite. A reinforcement of 1, 2 and 3 vol% TiO_2 nanoparticles led to increases of 57, 42 and 41%, respectively, in the fracture toughness compared with the original polyester. However, a 4 vol% TiO_2 reinforcement decreased the toughness value (0.55 MPam $^{1/2}$) to approximately the value of the original polyester matrix (0.54 MPam $^{1/2}$). This variation can be explained by observing the TEM images shown in Fig. 22. It is clear from the TEM images that the nanocomposites containing 1, 2 and 3 vol% TiO_2 show excellent particle dispersion stability. However,

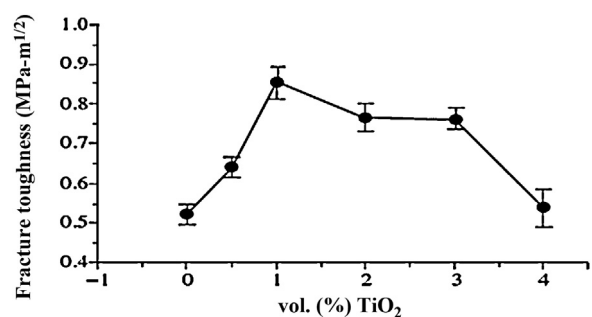


Fig. 21. Variation of quasi-static fracture toughness as a function of volume fraction of TiO_2 nanoparticles in the polyester/ TiO_2 nanocomposite. Reprinted from [269], Copyright 2003, with permission from Elsevier.

agglomeration was observed in the samples containing 4 vol% TiO_2 due to weak bonding between the titania particles and the polyester, which results in a decline in the fracture toughness [269].

Zhang and Yang [312] reported that reinforcement by TiO_2 nanoparticles improves the poor creep resistance and the dimensional stability of PA6,6 thermoplastic composites. Chisholm et al. [313] studied the effect of micro- and nano-sized SiC reinforcement on the mechanical properties of an epoxy matrix system and found that nanoparticle-based composites have superior thermal and mechanical properties compared to microsized particle-based composites. Ng et al. [314] found that a 10 wt% loading of TiO_2 nanoparticles in epoxy improves the scratch resistance and the toughness of the epoxy composites when compared with either micro-particle filled epoxy or pure epoxy. Rong et al. [315] performed tribological experiments on nano- TiO_2 /epoxy composites and found that the performance significantly depended on the dispersion state and microstructural homogeneity of the fillers. Schwartz and Bahadur [316] studied the tribological behavior and

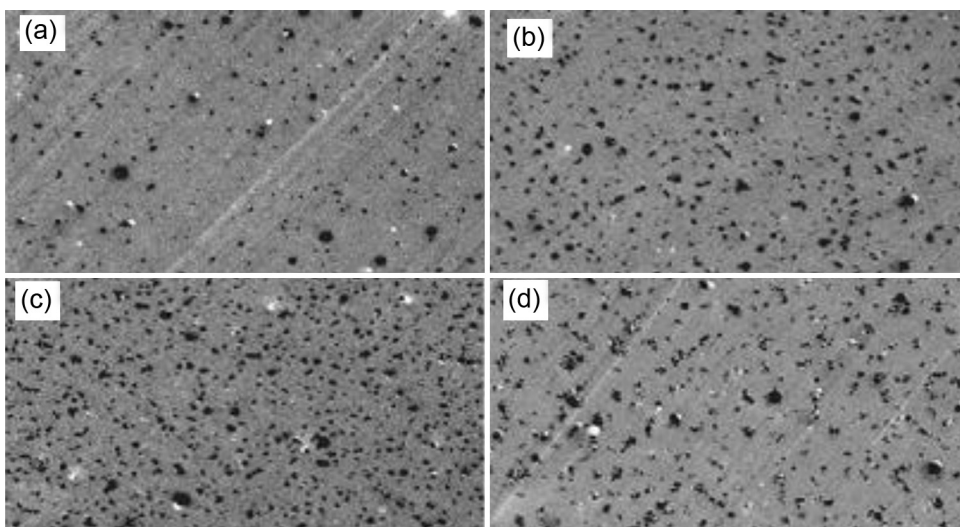


Fig. 22. TEM micrographs depicting the level of TiO_2 nanoparticle dispersion within the polyester matrix in the polyester/ TiO_2 nanocomposite. Volume fraction of particles: (a) 1 vol.%; (b) 2 vol.%; (c) 3 vol.%; and (d) 4 vol.%. Reprinted from [269], Copyright 2003, with permission from Elsevier.

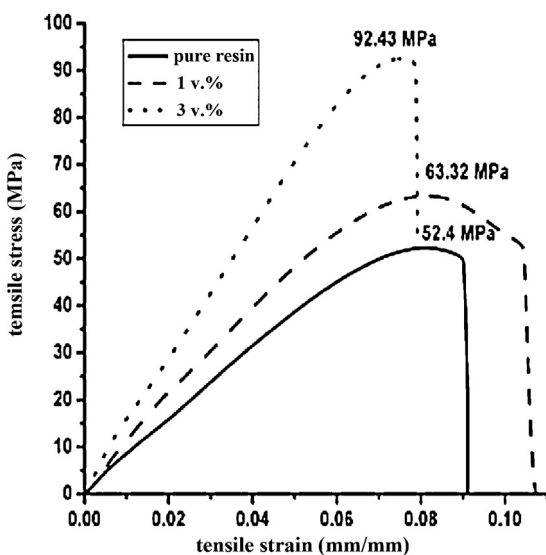


Fig. 23. Stress–strain curves of the cured pure resin 1 vol%, and 3 vol% functionalized nanoparticle filled nanocomposites.

Reprinted from [179], Copyright 2006, with permission from Royal Society of Chemistry.

the transfer-film counterface bond strength of nano-alumina/PPS composites. The results showed that the composites with 2 vol% filler loading have the lowest wear rate and strong bond strength while further increases in filler content lead to higher wear rates. The interpretation of the authors was that nanoparticles have the ability to anchor the transfer film to the counterface and thereby increase the bond strength, which lowers the wear. Siegel et al. [317] studied the mechanical properties of silane-modified Al_2O_3 nanoparticle filled PMMA composites and found that 5 wt% loading of alumina nanoparticles in PMMA caused an increase in strain-to-failure of over 28%, which enabled ductile flow in the glassy state. Guo et al. [179] measured the tensile modulus and the strength of pure resin and alumina-filled nanocomposites using microtensile tests. Fig. 23 shows the resulting stress–strain curves. The addition of MPS-modified alumina nanoparticles increased both the tensile modulus and the strength. The toughness, i.e., the area under the stress–strain curve before rupture, also increased significantly. Fig. 24 shows the tensile strength (the maximum stress in the stress–strain curve in MPa) and Young's modulus (the slope of the stress–strain curve in the low strain region) as a function of nanoparticle volume content. The tensile strength and Young's modulus of the 3 vol% filled nanocomposite increased by approximately 60% and 85%, respectively, compared with pure resin. Silane modification of the nanoparticles was observed to have little effect on the Young's modulus compared with unmodified particle-filled nanocomposites.

5.2.2. Optical properties

Useful optical properties and applications of PINCs, including light absorption (UV and visible), photoluminescence, extreme refractive index, and dichroism, have made PINCs an important class of functional materials for centuries. The optical properties of these PINC

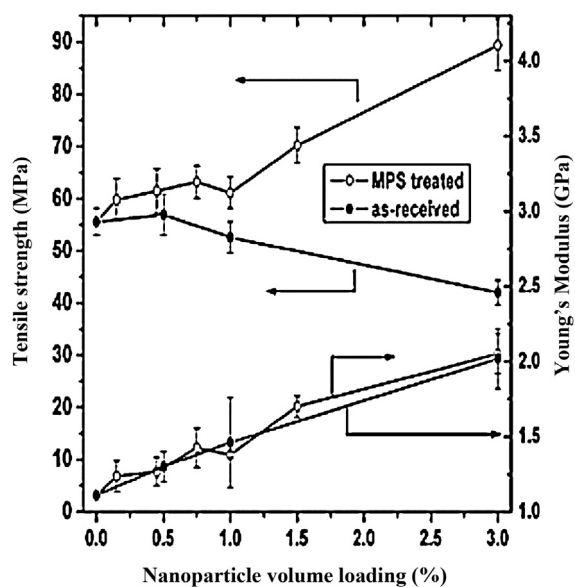


Fig. 24. Tensile strength and Young's modulus as a function of nanoparticle volume loading.

Reprinted from [179], Copyright 2006, with permission from Royal Society of Chemistry.

composites depend upon the size and spatial distribution of inorganic particles in the polymer matrix [12]. PINCs that consist of polymer and inorganic UV-absorbers (ZnO and TiO_2) have been synthesized by direct addition of nano-fillers into polymer matrices [318,319]. For example, Fig. 25 shows that PMMA-ZnO nanocomposites have a pronounced UV-blocking effect even at low concentrations of the ZnO filler (0.017 wt%), but retain high transparency in the visible range even at bulk sizes (1 cm thick). Moreover, the PMMA-ZnO nanocomposites show much higher UV-shielding efficiency than commercially available UV-blocking contact lenses as they have approximately zero transmission in the range from 290 to 340 nm [284,320].

Ritzhaupt-Kleissl et al. [321] investigated the effect of surface modification of alumina nanoparticles on its

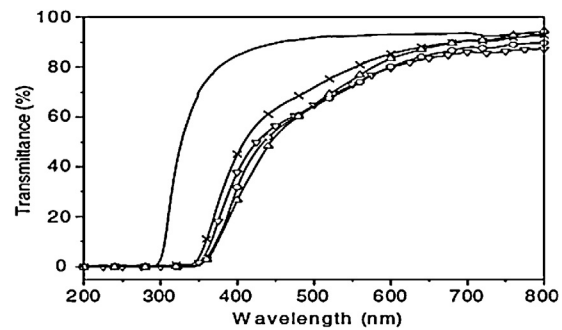


Fig. 25. UV-VIS spectra of PMMA-ZnO nanocomposites as synthesized by in situ sol-gel polymerization (ZnO content: * 0 wt%; X 0.017 wt%; ▽ 0.026 wt%; Δ 0.040 wt%; ○ 0.050 wt%, the thickness of all the samples is 1 cm).

Reprinted from [320], Copyright 2007, with permission from John Wiley and Sons and from [284], Open access, 2010.

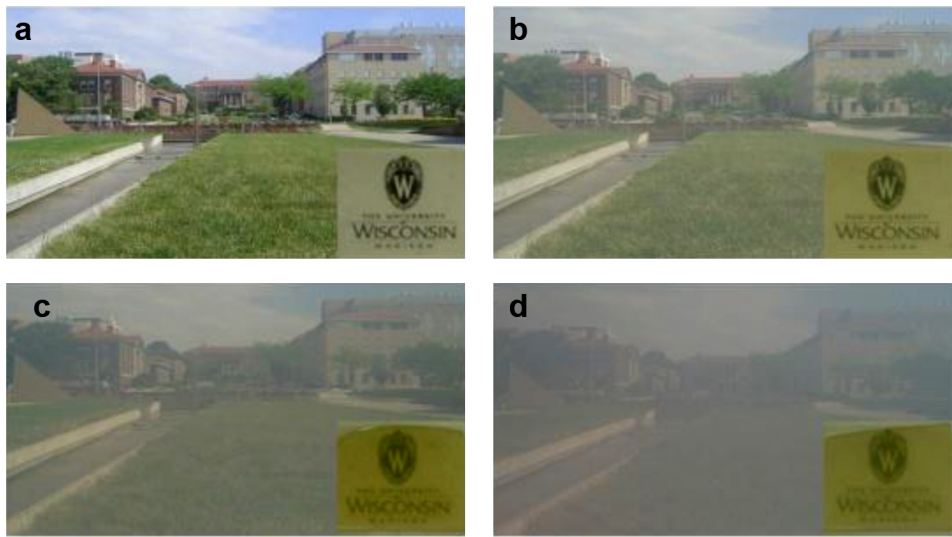


Fig. 26. Transparencies of the (a) PC neat resin, (b) 1 wt% and (c) 2 wt% PC/alumina (SMA-coated), and (d) 2 wt% PC/alumina (untreated). Reprinted from [338], Copyright 2008, with permission from Elsevier.

optical properties. Silane-treated Al_2O_3 nanoparticles dispersed in PMMA resin had an altered refractive index and yielded better optical transmittance values in the visible and infrared regions when compared with unmodified Al_2O_3 nanoparticles. Althues et al. [322] observed that the excitation and emission wavelengths of ZnO/polybutanediolmonoacrylate nanocomposites increased with an increase in ZnO particle size 6 to 10 nm. Sun and Sue [323] also reported similar results for ZnO quantum dots dispersed in a PMMA matrix. Du et al. [324] studied the photoluminescence properties of ZnO nanoparticles embedded in a PMMA matrix. They found that the ZnO nanoparticles (5–6 nm) embedded in PMMA exhibited UV emission at 334 nm due to quantum size effects in the nanoparticles and photoluminescence at 346 nm due to the presence of bound excitons in R-(COO)-ZnO complexes. The same mechanism has also been reported for luminescent oxide/PMMA nanocomposites in other studies [325–327]. Peres et al. [328] observed a bright green photoluminescence at 2.29 eV for CdSe/polybutylacrylate (PBA) nanocomposites under UV excitation. The core/shell nanoparticles made of HfO_2 , ZrO_2 , Al_2O_3 , or ZnO cores and a PMMA shell also exhibited strong luminescence [325,327]. The non-conducting oxide/polymer nanoparticles exhibit luminescence due to the presence of carboxylate groups at the interface between the ceramic and the PMMA whereas semiconductor nanoparticles, such as ZnO, show inherent luminescence [326]. The photoluminescent nanocomposites show great potential for application in various fields. For example, ZnO-based epoxy nanocomposites can be used for solid state lighting [329], and polymer core/shell composites containing ZnO nanoparticles can be used for *in vitro* cell imaging [330].

The refractive index (RI) of polymeric nanocomposites can be controlled by the addition of inorganic nanoparticles into the polymer matrix. Nanocomposite materials with enhanced RI find potential applications in lenses, optical filters, reflectors, optical waveguides, optical adhesives, solar

cells, or antireflection films [331]. The inorganic nanoparticles that are generally used to improve the refractive index of polymer nanocomposites include lead sulphide (PbS) [332], zinc sulphide (ZnS) [333], and iron sulphide (FeS) [334]. Lu et al. [333] reported that a loading of 50 wt% ZnS nanoparticles increased the RI of poly(*N,N*-dimethylacrylamide) composite from 1.54 to 1.63. Chau et al. [335] reported that a reinforcement of 30 wt% TiO_2 nanoparticles into the epoxy resin results in the formation of an epoxy/ TiO_2 nanocomposite coating with a refractive index of 1.668. They also observed that several nanocomposite coatings with different percentages of TiO_2 nanoparticles exhibited remarkable optical transparencies of greater than 90%. Wang et al. [336] synthesized PMMA/ SiO_2 and PMMA/ ZrO_2 nanocomposites by a non-hydrolytic sol-gel method and studied their optical properties. They found that the transmittance of the nanocomposite films in the visible region remained above 95% even at a loading of 20 wt% inorganic nanoparticles, and the value increased proportionally with decreasing inorganic nanoparticle concentration. The pure polyamide and hybrid films filled with different concentrations of silica nanoparticles are both transparent, but the maximum transmittance was found in a hybrid film loaded with 5 wt% silica nanoparticles; further increases in silica content decreased the transmittance of the composite gradually [337]. Chandra et al. [338] discovered that the presence of alumina nanoparticles in polycarbonate (PC)/alumina nanocomposites reduced the overall light transmittance of the nanocomposites. The decrease in light transmittance was attributed to an increase in the loading of nanoparticles. The authors also observed that the poly(styrene-maleic anhydride) copolymer (SMA) treated alumina/PC nanocomposite exhibited a higher light transmittance than that of the untreated alumina/PC nanocomposite (Fig. 26).

Mallakpour and Barati [180] also reported a reduction in the overall light transmittance of the nanocomposites in

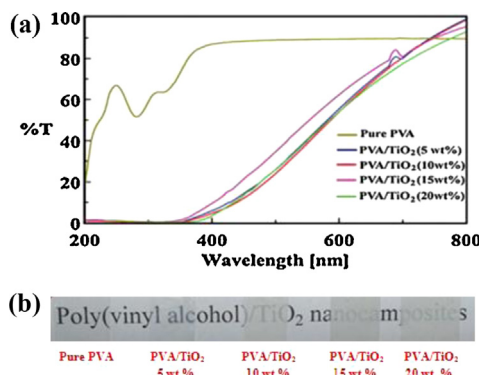


Fig. 27. UV-vis transmittance spectra of (a) pure PVA film and of PVA/TiO₂ nanocomposite films. (b) Visual transparencies of the pure PVA and PVA/TiO₂ nanocomposite films.

Reprinted from [180], Copyright 2011, with permission from Elsevier.

the presence of TiO₂ nanoparticles as shown in Fig. 27a. Increased TiO₂ nanoparticle content decreased the light transmittance to a further extent. However, the nanocomposite exhibits absorption in the UV region, so this type of nanocomposite film could be used as a UV-shielding coating. Fig. 27b shows that the PVA/TiO₂ 5 wt% nanocomposite was the most transparent although some haziness can still be observed, and even the 10 wt% nanocomposite is still relatively transparent.

5.2.3. Magnetic properties

Magnetic nanocomposites are from one of two groups: those containing metal nanoparticles and those containing Fe₂O₃, Fe₃O₄ or ferrite nanoparticles. Most of the nanocomposites resulting from ferrite or metal nanoparticles are free of hysteresis, which indicates a superparamagnetic material. Ziolo et al. [339,340] observed that a polymer nanocomposite filled with 21.8 wt% Fe₂O₃ nanoparticles showed a saturation magnetization of 15 Am²/kg. The nanocomposite was free of hysteresis at room temperature and also exhibited optical transparency. A saturation magnetization of 58 Am²/kg was observed for a composite of magnetic Fe₂O₃ nanoparticles and electroconducting polypyrrole [341]. Zhan et al. [342] observed superparamagnetic behavior in PI/γ-Fe₂O₃ nanocomposite films and also observed an increase from 1.354×10^{-2} A to 4.220×10^{-2} A in the saturation magnetization of the PI/γ-Fe₂O₃ nanocomposite films with an increase in the Fe₃O₄ loading content from 2 wt% to 8 wt%. Thus, the magnetic properties of nanocomposites can be controlled by varying the Fe₃O₄ loading content. Fig. 28 shows the magnetic hysteresis loops of the polypyrrole nanocomposites filled with 20 and 50 wt% loading of iron oxide nanoparticles. The samples formed from the 7 h reaction do not show any hysteresis, which is attributed to the dissolution of the magnetic nanoparticles in the acidic medium. The saturation magnetizations (Ms) with an initial loading of 20 and 50 wt% of particles were found to be 29.4 emu/g and 45.1 emu/g, respectively. A saturation magnetization of 74 emu/g has been reported for iron oxide nanoparticles, and that value was independent of the surface chemistry of the nanoparticles [343].

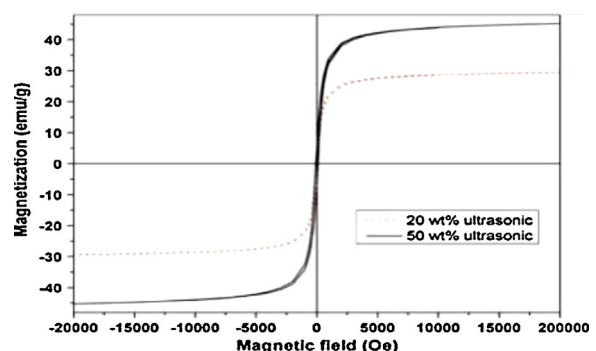


Fig. 28. Magnetic hysteresis loops of nanocomposites at different loadings.

Reprinted from [343], Copyright 2009, with permission from Springer.

5.2.4. Electrical properties

Polymer-inorganic nanocomposites have been in a close relationship with the design of advanced electronic and optoelectronic devices. The dimensional scale for electronic devices has now entered the nano-range. Su and Kuramoto [344] reported the synthesis of PANi/TiO₂ nanocomposites by in situ polymerization of PANi in the presence of TiO₂ nanoparticles. The as-synthesized nanocomposite films showed appreciable conductivity (1–10 S/cm), which was further increased by thermal treatment at 80 °C for 1 h. Mo et al. [345] also carried out the synthesis of PANi/TiO₂ nanocomposites using TiO₂ nanoparticles and colloids. The dielectric constant and loss also increased with increased TiO₂ loading. The conductivity of the nanocomposites also gradually increased as the amount of TiO₂ increased from 1 to 5 wt%. Ma et al. [286] reported that the surface resistivity of polystyrene resin/ZnO nanocomposites synthesized by melt-blending decreases as the concentration of ZnO increases. The addition of 30 wt% of either ZnO spherical particles or whiskers also caused a reduction in the surface resistivity of the composite materials from 1.0×10^{16} to $8.98 \times 10^{12} \Omega/\text{cm}^2$ and $9.57 \times 10^{10} \Omega/\text{cm}^2$, respectively. The amount of ZnO in the polystyrene resin can be gradually increased to form a conductive network. Ma et al. [346] observed that functionalization of TiO₂ nanoparticles improves the electrical properties of polyethylene/TiO₂ nanocomposites. Singha and Thomas [347] investigated the dielectric properties of epoxy nanocomposites containing TiO₂, ZnO and Al₂O₃ nano-fillers at low filler concentrations by weight and observed some unique electrical properties that could be advantageous in several existing and potential electrical systems.

5.2.5. Thermal properties

Thermal properties are those material properties that change with temperature. They can be studied by thermal analysis techniques including DSC, TGA, DTA, TMA, DMA/DMTA, and dielectric thermal analysis. The incorporation of nanometer-sized inorganic particles into the polymer matrix can enhance thermal stability by acting as a superior thermal insulator and as a mass transport barrier to the volatile products generated during decomposition [348]. Tang et al. [220] reported that the thermal stability

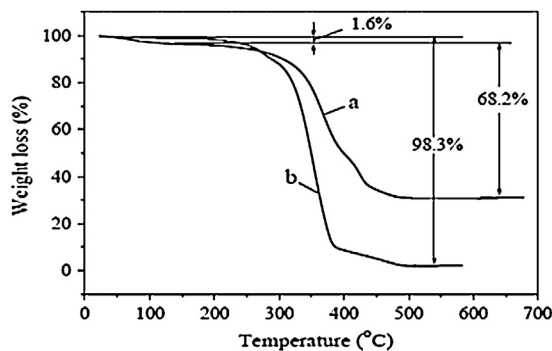


Fig. 29. The weight loss curves of (a) composite particles and (b) pure polymer.
Reprinted from [220], Copyright 2006, with permission from Elsevier.

of P(MMA–MAA)/nano-ZnO nanocomposites is superior to that of pure P(MMA–MAA); the higher thermal decomposition is illustrated in Fig. 29.

Chen et al. [349] observed that minimal loading (5 wt%) of an Al₂O₃ nanofiller induced a higher thermal stability whereas larger Al₂O₃ concentrations (9 wt%) caused a marked weight loss even at low temperatures. Similar behavior was observed for the glass transition temperature (TG). Omrani et al. [350] also observed that the TG increased at up to 5 wt% loading of Al₂O₃ fillers. An increase in TG and a reduction in the coefficient of thermal expansion (CTE) were also reported in epoxy composites filled with surface-modified nano-SiO₂ monospheres

[351]. Wu and Ke [352] discovered that PS-encapsulated SiO₂ nanoparticles enhance the crystallization of PET compared to both unmodified SiO₂ and modified SiO₂. The PET-SiO₂/PS nanocomposite films that have a 2 wt% loading of PS-encapsulated SiO₂ nanoparticles also have the highest crystallization rate. This may be due to the nucleation effect of PS-encapsulated SiO₂ nanoparticles in the PET matrix. Wang et al. [336] reported that decomposition temperatures in PMMA/SiO₂ and PMMA/ZrO₂ nanocomposites increased significantly in cases where the maximum weight loss was observed by thermal decomposition of PMMA segments. The authors attributed this phenomenon to the fact that the thermal decomposition temperatures of PMMA/SiO₂ and PMMA/ZrO₂ had increased because the network structure between the inorganic and organic components reduces the movement of polymer chains, and inorganic components may blunt the attack of free radicals. Laachachi et al. [353] reported an improvement in the thermal stability of PMMA/oxide nanocomposites by reinforcements from ferric-oxide and zinc-oxide nanoparticles. Guo et al. [343] revealed that the thermal stability and decomposition temperatures of Fe₂O₃/PPy nanocomposites increased slightly with increasing nanoparticle loading.

5.3. Applications of organic–inorganic nanocomposites

The incorporation of inorganic nanofiller into organic matrices provides superior mechanical, optical, electronic and thermal properties for the resulting organic–inorganic nanocomposite materials. The improvements in these

Table 3
Potential applications of organic–inorganic nanocomposites.

Nanocomposites	Applications	References
PMMA/SiO ₂	Bioactive bone substitute, Dental application and optical devices	[354,355]
Polycaprolactone/SiO ₂	Bone-bioerodible for skeletal tissue repair	[355]
Polyimide/SiO ₂	Microelectronics.	[355]
Polyethylacrylate/SiO ₂	Catalysis support, stationary phase for chromatography	[355]
Poly(p-phenylene vinylene)/SiO ₂	Non-linear optical material for optical waveguides.	[355]
Polyaniline/Fe ₃ O ₄	Microwave absorber	[356]
Poly(N-isopropylacrylamide)/Magnetic SBA-15	Drug delivery	[357]
Polyethylenimine/Iron oxide	Magnetic resonance imaging	[358]
High-density polyethylene/TiO ₂	Bone repair	[359]
Poly(amide-imide)/TiO ₂	Composite membranes for gas separation.	[355]
Low density polyethylene/ZnO/Ag	Orange juice packaging,	[360]
Poly(3,4-ethylene-dioxythiphene)/V ₂ O ₅	Cathode materials for rechargeable lithium batteries.	[361]
Polycarbonate/SiO ₂	Abrasion resistant coating.	[361]
Shape memory polymers/SiC	Medical devices for gripping or releasing therapeutics within blood vessels.	[355]
Nylon-6/LS	Automotive timing-belt-TOKYOTA.	[355]
Nylon-6/clay	Barrier films – Bayer AG	[355,361]
Nylon-6/clay	Films and bottles – Honeywell	[361]
Nylon-6, 12, 66/clay	Auto fuel systems – Ube	[361]
Nylon-6/PP/clay	Electrically conductive	[361]
UHMWPE/clay	Earthquake-resistance pipes – Yantai Haili Ind.& Commerce of China 305	[361]
Polypropylene/clay	Packaging – Clariant	[361]
PEO/LS	Airplane interiors, fuel tanks, components in electrical and electronic parts, brakes and tires.	[355]
PET/clay	Food packaging application. Specific examples include packaging for processed meats, cheese, confectionery, cereals and boil-in-the-bag foods, fruit juice and dairy products, beer and carbonated drinks bottles.	[355]
Polyimide/clay	Automotive step assists – GM Safari and Astra Vans.	[355]
Epoxy/MMT	Materials for electronics.	[355]
SPEEK/laponite	Direct methanol fuel cells.	[355]
EVA/clay	Wires and cables – Kabelwerk Eupen of Belgium	[361]
Unsaturated polyester/clay	Marine, transportation – Polymeric Supply	[361]

material properties have resulted in the application of these composites in many fields, such as optics, electronics, mechanics, energy, environment, biology and medicine. Nanocomposite materials may be used in membranes and separation devices, functional smart coatings, fuel and solar cells, catalysts, sensors, military equipment, antimicrobial textiles and paints, automobiles, aerospace, drug carriers and tissue engineering. Furthermore, the superior mechanical properties of polymer nanocomposites allows them to be used in many general and industrial applications, which include impellers and blades for vacuum cleaners, power tool housings, mower hoods, covers for portable electronic equipment, such as mobile phones and pagers and glues for the manufacturing of pressure molds in the ceramic industry. Among polymer–inorganic nanocomposites, the SiO₂, TiO₂, ZnO and clay-based nanocomposites have been most widely studied because of their potential application in various fields. For example, polymer–SiO₂ nanocomposites are used in optical devices, in microelectronics and as a bioactive bone substitute [354,355]. Magnetic nanocomposites find applications in microwave absorption, drug delivery and magnetic resonance imaging [356–358]. Polymer–TiO₂ nanocomposites have been used in bone repair and in composite membranes for gas separation [355,359], and polymer–ZnO nanocomposites can be used in food packaging due to their antibacterial properties [360]. Polymer–clay nanocomposites are widely used in barrier films, wires and cables, auto fuel systems and food packaging [355,361]. Some of the potential applications of polymer inorganic nanocomposites are listed in Table 3.

6. Conclusions

Organic–inorganic nanocomposite materials possess unique properties as new materials and compounds for academic research as well as for the development of innovative industrial applications. These nanocomposites combine the unique properties of organic and inorganic components in one material. The basic multifunctional feature of these nanocomposite materials makes them potentially applicable in various areas in high added-value applications such as smart coatings for corrosion protection and abrasion resistance; artificial membranes for ultra- and nanofiltration, pervaporation and gas separation; catalysts and nanoscopic reactors; adsorbents of toxic metal ions; biomaterials for osteo-reconstructive surgery; or ophthalmic devices with optoelectronic and magnetic properties for telecommunications or information displays. In developing these composites, the inorganic nanoparticles have a strong tendency to form aggregates; therefore, to improve the dispersion stability and compatibility of inorganic nanofillers with organic solvents or polymer matrices, their surfaces should be modified either by grafting polymers or by absorption of small molecules, such as silane coupling agents. Surface modification improves the interfacial interactions between the inorganic nanofillers and polymer matrices, which results in unique properties, such as very high mechanical toughness (even at low loadings of inorganic reinforcements) and other optical, electronic, gas-barrier and flame-retardance properties.

Thus, the surface modification of inorganic nanofillers is necessary to produce high-performance organic–inorganic nanocomposite materials.

References

- [1] Jeon IY, Baek JB. Nanocomposites derived from polymers and inorganic nanoparticles. *Materials* 2010;3:3654–74.
- [2] Skaff H, Emrick T. Reversible addition fragmentation chain transfer polymerization from the surface of unprotected CdSe nanoparticles. *Angewandte Chemie International Edition* 2004;43:5383–6.
- [3] Peng Q, Lai DMY, Kang ET, Neoh KG. Preparation of polymer–silicon (100) hybrids via interface-initiated reversible addition–fragmentation chain-transfer (RAFT) polymerization. *Macromolecules* 2006;39:5577–82.
- [4] Taniguchi Y, Ogawa M, Gang W, Saitoh H, Fujiki K, Yamauchi T, et al. Preparation of hyperfunctional carbon black by grafting of hyperbranched polyester onto the surface. *Materials Chemistry and Physics* 2008;108:397–402.
- [5] Walter R, Friedrich K, Privalko V, Savadori AJ. On modulus and fracture toughness of rigid particulate filled high density polyethylene. *Journal of Adhesion* 1997;64:87–109.
- [6] Breiner JM, Mark JE. Preparation, structure, growth mechanisms and properties of siloxane composites containing silica, titania or mixed silica–titania phases. *Polymer* 1998;39:5486–93.
- [7] Rong MZ, Zhang MQ, Zheng YX, Zeng HM, Friedrich K. Improvement of tensile properties of nano-SiO₂/PP composites in relation to percolation mechanism. *Polymer* 2001;42:3301–4.
- [8] Yang H, Zhang Q, Guo M, Wang C, Du NR, Fu Q. Study on the phase structures and toughening mechanism in PP/EPDM/SiO₂ ternary composites. *Polymer* 2006;47:2106–15.
- [9] Kruenate J, Tongpool R, Panyathanaporn T. Optical and mechanical properties of polypropylene modified by metal oxides. *Surface and Interface Analysis* 2004;36:1044–7.
- [10] Bao SP, Tjong SC. Impact essential work of fracture of polypropylene/montmorillonite nanocomposites toughened with SEBS-g-MA elastomer. *Composites Part A: Applied Science and Manufacturing* 2007;38:378–87.
- [11] Caseri W. Nanocomposites of polymers and metals or semiconductors historical background and optical properties. *Macromolecular Rapid Communications* 2000;21:705–22.
- [12] Caseri W. Inorganic nanoparticles as optically effective additives for polymers. *Chemical Engineering Communications* 2009;196:549–72.
- [13] Okada A, Usuki A. Twenty years of polymer-clay nanocomposites. *Macromolecular Materials and Engineering* 2006;291:1449–76.
- [14] Allemann E, Gurny R, Doelker E. Drug loaded nanoparticles preparation methods and drug targeting issues. *European Journal of Pharmaceutics and Biopharmaceutics* 1993;39:173–91.
- [15] Golander CG, Herron JN, Lim K, Claesson P, Stenius P, Andrade JD. Properties of immobilized PEG films and the interaction with proteins: experiments and modeling. In: Harris JM, editor. *Poly(ethylene glycol) chemistry, biotechnical and biomedical applications*. New York: Plenum Press; 1992. p. 221–45.
- [16] Masala O, Seshadri R. Synthesis routes for large volumes of nanoparticles. *Annual Review of Materials Research* 2004;34:41–81.
- [17] Chen HM, Liu RS. Architecture of metallic nanostructures: synthesis strategy and specific applications. *Journal of Physical Chemistry C* 2011;115:3513–27.
- [18] Hanemann T, Szabo DV. Polymer-nanoparticle composites: from synthesis to modern applications. *Materials* 2010;3:3468–517.
- [19] Jitputti J, Rattanavoravipa T, Chuangchote S, Pavasupree S, Suzuki Y, Yoshikawa S. Low temperature hydrothermal synthesis of monodispersed flower-like titanate nanosheets. *Catalysis Communications* 2009;10:378–82.
- [20] Mizukoshi Y, Makise Y, Shuto THJ, Tominaga A, Shironita S, Tanabe S. Immobilization of noble metal nanoparticles on the surface of TiO₂ by the sonochemical method: photocatalytic production of hydrogen from an aqueous solution of ethanol. *Ultrasonics Sonochemistry* 2007;14:387–92.
- [21] Zhang Y, Zheng H, Liu G, Battaglia V. Synthesis and electrochemical studies of a layered spheric TiO₂ through low temperature solvothermal method. *Electrochimica Acta* 2009;54:4079–83.
- [22] Li XL, Peng Q, Yi JX, Wang X, Li Y. Near monodisperse TiO₂ nanoparticles and nanorods. *Chemistry: A European Journal* 2006;12:2383–91.

- [23] Zhang DB, Qi LM, Cheng HM, Ming JMA. Synthesis of crystalline nanosized titanium dioxide via a reverse micelle method at room temperature. *Chinese Chemical Letters* 2003;14:100–3.
- [24] Anwar NS, Kassim A, Lim HN, Zakarya SA, Huang NM. Synthesis of TiO₂ nanoparticles via sucrose ester micelle-mediated hydrothermal processing route. *Sains Malays* 2010;39:261–5.
- [25] Rahim S, Radiman S, Hamzah A. Inactivation of *Escherichia coli* under fluorescent lamp using TiO₂ nanoparticles synthesized via sol gel method. *Sains Malays* 2012;41:219–24.
- [26] Yang H, Zhang K, Shi R, Li X, Dong X, Yu Y. Sol-gel synthesis of TiO₂ nanoparticles and photocatalytic degradation of methyl orange in aqueous TiO₂ suspensions. *Journal of Alloys and Compounds* 2006;413:302–6.
- [27] Jagadale TC, Takale SP, Sonawane RS, Joshi HM, Patil SI, Kale BB, et al. N-doped TiO₂ nanoparticle based visible light photocatalyst by modified peroxide sol-gel method. *Journal of Physical Chemistry C* 2008;112:14595–602.
- [28] Teleki A, Pratsinis SE, Kalyanasundaram K, Gouma PI. Sensing of organic vapors by flame-made TiO₂ nanoparticles. *Sensors and Actuators B* 2006;119:683–90.
- [29] Parala H, Devi A, Bhakta R, Fischer RA. Synthesis of nano-scale TiO₂ particles by a nonhydrolytic approach. *Journal of Materials Chemistry* 2002;12:1625–7.
- [30] Zhao Y, Li C, Liu X, Gu F, Jiang H, Shao W, et al. Synthesis and optical properties of TiO₂ nanoparticles. *Materials Letters* 2007;61:79–83.
- [31] Barnard AS, Erdin S, Lin Y, Zapol P, Halley JW. Modeling the structure and electronic properties of TiO₂ nanoparticles. *Physical Review B* 2006;73:205405/1–8.
- [32] Auvinen S, Alatalo M, Haario H, Jalava JP, Lamminmaki RJ. Size and shape dependence of the electronic and spectral properties in TiO₂ nanoparticles. *Journal of Physical Chemistry C* 2011;115:8484–93.
- [33] Hoang VV, Zung H, Trong NHB. Structural properties of amorphous TiO₂ nanoparticles. *European Physical Journal D* 2007;44:515–24.
- [34] Shao W, Nabb D, Renevier N, Sherrington I, Fu Y, Luo J. Mechanical and anti-corrosion properties of TiO₂ nanoparticle reinforced Ni coating by electrodeposition. *Journal of the Electrochemical Society* 2012;159:671–6.
- [35] Carp O, Huisman CL, Reller A. Photoinduced reactivity of TiO₂. *Progress in Solid State Chemistry* 2004;32:33–177.
- [36] Lee KM, Hu CW, Chen HW, Ho KC. Incorporating carbon nanotube in a low-temperature fabrication process for dye-sensitized TiO₂ solar cells. *Solar Energy Materials and Solar Cells* 2008;92:1628–33.
- [37] Mohammadi MR, Fray DJ, Cordero-Cabrera MC. Sensor performance of nanostructured TiO₂ thin films derived from particulate sol-gel route and polymeric fugitive agents. *Sensors and Actuators B* 2007;124:74–83.
- [38] Wang YQ, Zhang HM, Wang RH. Investigation of the interaction between colloidal TiO₂ and bovine hemoglobin using spectral methods. *Colloids and Surfaces B* 2008;65:190–6.
- [39] Chen X, Mao SS. Titanium dioxide nanomaterials: synthesis, properties, modification and applications. *Chemical Reviews* 2007;107:2891–959.
- [40] Adesina AA. Industrial exploitation of photocatalysis progress, perspectives and prospects. *Catal Surv Asia* 2004;8:265–73.
- [41] Chitose N, Ueta S, Yamamoto TA. Radiolysis of aqueous phenol solutions with nanoparticles: phenol degradation and TOC removal in solutions containing TiO₂ induced by UV, gamma-ray and electron beams. *Chemosphere* 2003;50:1007–13.
- [42] Kabra K, Chaudhary R, Sawhney RL. Treatment of hazardous organic and inorganic compounds through aqueous-phase photocatalysis: a review. *Industrial and Engineering Chemistry Research* 2004;43:7683–96.
- [43] Kuhn KP, Caherny IF, Massholder K, Stickler M, Benz VW, Sonntag H, et al. Disinfection of surfaces by photocatalytic oxidation with titanium dioxide and UVA light. *Chemosphere* 2003;53:71–7.
- [44] Choi JY, Kim KH, Choy KC, Oh KT, Kim KN. Photocatalytic antibacterial effect of TiO₂ film formed on Ti and Ti/Ag exposed to *Lactobacillus acidophilus*. *Journal of Biomedical Materials Research Part B: Applied Biomaterials* 2007;80:353–9.
- [45] Chu SY, Yan TM, Chen SL. Analysis of ZnO varistors prepared by the sol-gel method. *Ceramics International* 2000;26:733–7.
- [46] Westin G, Ekstrand A, Nygren M, Sterlund RO, Merkelbach P. Preparation of ZnO-based varistors by the sol-gel technique. *Journal of Materials Chemistry* 1994;4:615–21.
- [47] Tokumoto MS, Briois V, Santilli CV. Preparation of ZnO nanoparticles and colon: structural study of the molecular precursor. *Journal of Sol-Gel Science and Technology* 2003;26:547–51.
- [48] Kim JH, Choi WC, Kim HY, Kang Y, Park YK. Preparation of mono-dispersed mixed metal oxide micro hollow spheres by homogeneous precipitation in a micro precipitator. *Powder Technology* 2005;153:166–75.
- [49] Damonte LC, Zelis LAM, Soucase BM, Fenollosa MAH. Nanoparticles of ZnO obtained by mechanical milling. *Powder Technology* 2004;148:15–9.
- [50] Kahn ML, Monge M. Size- and shape-control of crystalline zinc oxide nanoparticles: a new organometallic synthetic method. *Advanced Functional Materials* 2005;15:458–68.
- [51] Komarneni S, Bruno M, Mariani E. Synthesis of ZnO with and without microwaves. *Materials Research Bulletin* 2000;35:1843–7.
- [52] Zhao XY, Zheng BC, Li CZ, Gu HC. Acetate-derived ZnO ultrafine particles synthesized by spray pyrolysis. *Powder Technology* 1998;100:20–3.
- [53] Dai ZR, Pan ZW, Wang ZL. Novel nanostructures of functional oxides synthesized by thermal evaporation. *Advanced Functional Materials* 2003;13:9–24.
- [54] Padmavathy N, Vijayaraghavan R. Enhanced bioactivity of ZnO nanoparticles—an antimicrobial study. *Science and Technology of Advanced Materials* 2008;9, 035004/1–7.
- [55] Pillai SC, Kelly JM, McCormack DE, Ramesh R. Self-assembled arrays of ZnO nanoparticles and their application as varistor materials. *Journal of Materials Chemistry* 2004;14:1572–8.
- [56] Ao WQ, Li JQ, Yang HM, Zeng XR, Ma XC. Mechanochemical synthesis of zinc oxide nanocrystalline. *Powder Technology* 2006;168:148–51.
- [57] Kundu TK, Karki N, Barik P, Saha S. Optical properties of ZnO nanoparticles prepared by chemical method using poly (vinyl alcohol) (PVA) as capping agent. *International Journal of Soft Computing and Engineering* 2011;1:19–24.
- [58] Dakhlaoui A, Jendoubi M, Smiri LS, Kanaev A, Jouini N. Synthesis, characterization and optical properties of ZnO nanoparticles with controlled size and morphology. *Journal of Crystal Growth* 2009;311:3989–96.
- [59] Drath BE, Martin S, Mogens C, Brummerstedt IB. Particle size effects on the thermal conductivity of ZnO. *AIP Conference Proceedings* 2012;1449:335–8.
- [60] Singh AK. Synthesis, characterization, electrical and sensing properties of ZnO nanoparticles. *Advanced Powder Technology* 2010;21:609–13.
- [61] Carrey J, Kahn ML, Sanchez S, Chaudret B, Respaud M. Nanomaterials and nanotechnologies synthesis and transport properties of ZnO nanorods and nanoparticles assemblies. *The European Physical Journal Applied Physics* 2007;40:71–5.
- [62] Garcia MA, Merino JM, Pinel EF, Quesada A, de la Venta J, Gonzalez MLR, et al. Magnetic properties of ZnO nanoparticles. *Nano Letters* 2007;7:1489–94.
- [63] Ton-That C, Philips MR, Foley M, Moody SJ, Stampfli APJ. Surface electronic properties of ZnO nanoparticles. *Applied Physics Letters* 2008;92, 261916/1–3.
- [64] Chopra L, Major S, Pandya DK, Rastogi RS, Vankar VD. Thermal device applications. *Thin Solid Films* 1983;102:1:1–4.
- [65] Jiang P, Zhou JJ, Fang HF, Wang CY, Wang ZL, Xie SS. Hierarchical shelled ZnO structures made of bunched nanowire arrays. *Advanced Functional Materials* 2007;17:1303–10.
- [66] Chakrabarti S, Dutta BK. Photocatalytic degradation of model textile dyes in wastewater using ZnO as semiconductor catalyst. *Journal of Hazardous Materials B* 2004;112:269–78.
- [67] Chen C, Liu J, Liu P, Yu B. Investigation of photocatalytic degradation of methyl orange by using nano-sized ZnO Catalysts. *Advances in Chemical Engineering and Science* 2011;19:1–14.
- [68] Tan TK, Khiew PS, Chiu WS, Radiman S, Abd-Shukor R, Huang NM, et al. Photodegradation of phenol red in the presence of ZnO nanoparticles. *World Academy of Science, Engineering and Technology* 2011;79:791–6.
- [69] Zhou J, Xu N, Wang ZL. Dissolving behavior and stability of ZnO wires in biofluids: a study on biodegradability and biocompatibility of ZnO nanostructures. *Advanced Materials* 2006;18:2432–5.
- [70] Jones N, Ray B, Ranjit KT, Manna AC. Antibacterial activity of ZnO nanoparticle suspensions on a broad spectrum of microorganisms. *FEMS Microbiology Letters* 2008;279:71–6.
- [71] Jin T, Sun D, Su Y, Zhang H, Sue HJ. Antimicrobial efficacy of zinc oxide quantum dots against *Listeria monocytogenes*, *Salmonella enteritidis* and *Escherichia coli* O157:H7. *Journal of Food Science* 2009;74:46–52.
- [72] Ugur SS, Sariiskik M, Aktas AH, Ucar MC, Erden E. Modifying of cotton fabric surface with nano-ZnO multilayer films by layer-by-layer deposition method. *Nanoscale Research Letters* 2010;5:1204–10.

- [73] Li J, Guo D, Wang X, Wang H, Jiang H, Chen B. The photodynamic effect of different size ZnO nanoparticles on cancer cell proliferation in vitro. *Nanoscale Research Letters* 2010;5:1063–71.
- [74] Tok AIY, Boey FYC, Zhao XL. Novel synthesis of Al₂O₃ nano-particles by flame spray pyrolysis. *Journal of Materials Processing Technology* 2006;178:270–3.
- [75] Ke-long H, Liang-guo Y, Su-qin L, Chao-jian L. Preparation and formation mechanism of Al₂O₃ nanoparticles by reverse microemulsion. *The Transactions of Nonferrous Metals Society of China* 2007;17:633–7.
- [76] Macedo MIF, Osawa CC, Bertran CA. Sol-gel synthesis of transparent alumina gel and pure gamma alumina by urea hydrolysis of alumina nitrate. *Journal of Sol-Gel Science and Technology* 2004;30:135–40.
- [77] Karim MR, Rahman MA, Miah MAJ, Ahmad H, Yanagisawa M, Ito M. Synthesis of γ-alumina particles and surface characterization. *Open Colloid Science Journal* 2011;4:32–6.
- [78] Chang FY, Ning LG, Lin Y, Liu HC, Lin BY. A novel heat resisting surfactant for the modification of alumina nanoparticles. *Chinese Chemical Letters* 2003;14:104–7.
- [79] Nieto MI, Tallon C, Moreno R. Synthesis of gamma-alumina nanoparticles by freeze drying. *Advances in Science and Technology* 2006;45:223–30.
- [80] Gangwar J, Srivastava AK, Tripathi SK. Size-controlled synthesis and evaluation of optical properties of alumina nanoparticles. *AIP Conference Proceedings* 2011;1393:379–80.
- [81] Wong KFV, Kurma T. Transport properties of alumina nanofluids. *Nanotechnology* 2008;19, 345702/1–8.
- [82] Li G, Jiang A, Zhang L. Mechanical and fracture properties of nano-Al₂O₃ alumina. *Journal of Materials Science Letters* 1996;15:1713–5.
- [83] Sharma YC, Srivastava V, Upadhyay SN, Weng CH. Alumina nanoparticles for the removal of Ni(II) from aqueous solutions. *Industrial and Engineering Chemistry Research* 2008;47:8095–100.
- [84] Pacheco S, Medina M, Valencia F, Tapia J. Removal of inorganic mercury from polluted water using structured nanoparticles. *Journal of Environment Engineering* 2006;132:342–9.
- [85] Pakrashi S, Dalai S, Sabat D, Singh S, Chandrasekaran N, Mukherjee A. Cytotoxicity of Al₂O₃ nanoparticles at low exposure levels to a freshwater bacterial isolate. *Chemical Research in Toxicology* 2011;24:1899–904.
- [86] Jiang W, Mashayekhi H, Xing B. Bacterial toxicity comparison between nano- and micro-scaled oxide particles. *Environmental Pollution* 2009;157:1619–25.
- [87] Sadiq IM, Pakrashi S, Chandrasekaran N, Mukherjee A. Studies on toxicity of aluminium oxide (Al₂O₃) nanoparticles to microalgae species: *Scenedesmus* sp and *Chlorella* sp. *Journal of Nanoparticle Research* 2011;13:3287–99.
- [88] Becker S, Soukup JM, Gallagher JE. Differential particulate air pollution induced oxidant stress in human granulocytes, monocytes and alveolar macrophages. *Toxicology in Vitro* 2002;16:209–18.
- [89] Tepper F, Lerner M, Ginley D. Nanosized alumina fibers. *American Ceramic Society Bulletin* 2001;80:57–60.
- [90] Aghababazadeh R, Mirhabibi AR, Pourasad J, Brown A, Brydson A, Mahabad NA. Economical synthesis of nanocrystalline alumina using an environmentally low-cost binder. *Surface Science* 2007;601:2864–7.
- [91] Parveen S, Misra R, Sahoo SK. Nanoparticles: a boon to drug delivery, therapeutics, diagnostics and imaging. *Nanomedicine: Nanotechnology, Biology and Medicine* 2011;8:147–66.
- [92] Zawarha MF, El-Kheshen AA, Abd-El-Aal HM. Facile and economic synthesis of silica nanoparticles. *Journal of Ovonic Research* 2009;5:129–33.
- [93] Shekar S, Sander M, Riehl RC, Smith AJ, Braumann A, Kraft M. Modelling the flame synthesis of silica nanoparticles from tetraethoxysilane. *Chemical Engineering Science* 2012;70:54–66.
- [94] Aubert T, Grassel F, Mornet S, Duguel E, Cador O, Cordier S, et al. Functional silica nanoparticles synthesized by water-in-oil microemulsion processes. *Journal of Colloid and Interface Science* 2010;341:201–8.
- [95] Rahman IA, Padavettan V, Sipaut CS, Ismail J, Chee CK. Size-dependent physicochemical and optical properties of silica nanoparticles. *Materials Chemistry and Physics* 2009;114:328–32.
- [96] Rossi LM, Shi L, Quina FH, Rosenzweig Z. Stober synthesis of monodispersed luminescent silica nanoparticles for bioanalytical assays. *Langmuir* 2005;21:4277–80.
- [97] Rahman IA, Padavettan V. Synthesis of silica nanoparticles by sol-gel: size-dependent properties, surface modification, and applications in silica-polymer nanocomposites—a review. *Journal of Nanomaterials* 2012, 132424/1–15.
- [98] Anglin EJ. Porous silicon in drug delivery devices and materials. *Advanced Drug Delivery Reviews* 2008;60:1266–77.
- [99] Jia H. The structures and antibacterial properties of nano-SiO₂ supported silver/zinc silver materials. *Dental Materials* 2008;24:244–9.
- [100] Slowing BI, Trewyn BG, Giri S, Lin VSY. Mesoporous silica nanoparticles for drug delivery and biosensing applications. *Advanced Functional Materials* 2007;17:1225–36.
- [101] Jolivet JP, Chaneac C, Tronc E. Iron oxide chemistry: from molecular clusters to extended solid networks. *Chemical Communications* 2004;5:481–7.
- [102] Wan SR, Huang JS, Yan HS, Liu KL. Size-controlled preparation of magnetite nanoparticles in the presence of graft copolymers. *Journal of Materials Chemistry* 2006;16:298–303.
- [103] Zhou ZH, Wang J, Liu X, Chan HSO. Synthesis of Fe₃O₄ nanoparticles from emulsions. *Journal of Materials Chemistry* 2001;11:1704–9.
- [104] Albornoz C, Jacobo SE. Preparation of a biocompatible magnetic film from an aqueous ferrofluid. *Journal of Magnetism and Magnetic Materials* 2006;305:12–5.
- [105] Hou YL, Yu JF, Gao S. Solvothermal reduction synthesis and characterization of superparamagnetic magnetite nanoparticles. *Journal of Materials Chemistry* 2003;13:1983–7.
- [106] Pascal C, Pascal JL, Favier F, Payen C. Electrochemical synthesis for the control of gamma-Fe₂O₃ nanoparticle size, morphology, microstructure and magnetic behaviour. *Chemistry of Materials* 1999;11:141–7.
- [107] Franzel L, Bertino MF, Huba ZJ, Carpenter EE. Synthesis of magnetic nanoparticles by pulsed laser ablation. *Applied Surface Science* 2012;261:332–6.
- [108] Vijayakumar R, Koltypin Y, Felner I, Gedanken A. Sonochemical synthesis and characterization of pure nanometer sized Fe₃O₄ particles. *Materials Science and Engineering A* 2000;286:101–5.
- [109] Bandyopadhyay M, Bhattacharya J. Magnetic and calorific properties of magnetic nanoparticles: an equilibrium study. *Journal of Physics: Condensed Matter* 2006;18:11309–22.
- [110] Akbarzadeh A, Samiei M, Davaran S. Magnetic nanoparticles: physical properties, and applications in biomedicine. *Nanoscale Research Letters* 2012;7:144–56.
- [111] Martchenko I, Dietsch H, Moitzi C, Schurtenberger P. Hydrodynamic properties of magnetic nanoparticles with tunable shape anisotropy: prediction and experimental verification. *Journal of Physical Chemistry B* 2011;115:14838–45.
- [112] Roca AG, Costo R, Rebollo AF, Veintemillas-Verdaguer S, Tartaj P, Gonzalez-Carreno T, et al. Progress in the preparation of magnetic nanoparticles for applications in biomedicine. *Journal of Physics D* 2009;42, 224002/1–11.
- [113] Chan DCF, Kirpotin DB, Bunn PA. Synthesis and evaluation of colloidal magnetic iron oxides for the site-specific radiofrequency induced hyperthermia of cancer. *Journal of Magnetism and Magnetic Materials* 1993;122:374–8.
- [114] Babes L, Denizot B, Tanguy G, Le Jeune JJ, Jallet P. Synthesis of iron oxide nanoparticles used as MRI contrast agents: a parametric study. *Journal of Colloid and Interface Science* 1999;212:474–82.
- [115] Chertok B, Moffat BA, David AE, Yu F, Bergemann C, Ross BD, et al. Iron oxide nanoparticles as a drug delivery vehicle for MRI monitored magnetic targeting of brain tumors. *Biomaterials* 2008;29:487–96.
- [116] Khodabakhshi A, Amin MM, Mozaffari M. Synthesis of magnetite nanoparticles and evaluation of its efficiency for arsenic removal from simulated industrial wastewater. *Iranian Journal of Environmental Health Science & Engineering* 2011;8:189–200.
- [117] Tran N, Mir A, Mallik D, Sinha A, Nayar S, Webster TJ. Bactericidal effect of iron oxide nanoparticles on *Staphylococcus aureus*. *International Journal of Nanomedicine* 2010;5:277–83.
- [118] Yin H, Yamamoto T, Wada Y, Yanagida S. Large-scale and size-controlled synthesis of silver nanoparticles under microwave irradiation. *Materials Chemistry and Physics* 2004;83:66–70.
- [119] Pingali KC, Rockstraw DA, Deng S. Silver nanoparticles from ultrasonic spray pyrolysis of aqueous silver nitrate. *Aerosol Science and Technology* 2005;39:1010–4.
- [120] Lee I, Han SW, Kim K. Simultaneous preparation of SERS-active metal colloids and plates by laser ablation. *Journal of Raman Spectroscopy* 2001;32:947–52.
- [121] Long D, Wu G, Chen S. Preparation of oligochitosan stabilized silver nanoparticles by gamma irradiation. *Radiation Physics and Chemistry* 2007;76:1126–31.

- [122] Bonnemann H, Richards R. Nanoscopic metal particles—synthetic methods and potential applications. *European Journal of Inorganic Chemistry* 2001;10:2455–80.
- [123] Mallick K, Witcomb MJ, Scurrell MS. Polymer stabilized silver nanoparticles: a photochemical synthesis route. *Journal of Materials Science* 2004;39:4459–63.
- [124] Navaladian S, Viswanathan B, Viswanath R, Varadarajan T. Thermal decomposition as route for silver nanoparticles. *Nanoscale Research Letters* 2006;2:44–8.
- [125] Rodriguez-Sanchez L, Blanco MC, Lopez-Quintela MA. Electrochemical synthesis of silver nanoparticles. *Journal of Physical Chemistry B* 2000;104:9683–8.
- [126] Haes AJ, Van Duyne RP. A nanoscale optical biosensor: sensitivity and selectivity of an approach based on the localized surface plasmon resonance spectroscopy of triangular silver nanoparticles. *Journal of the American Chemical Society* 2002;124: 10596–604.
- [127] Gurunathan S, Lee KJ, Kalishwaralal K, Sheikpranbabu S, Vaideyanathan R, Eom SH. Antiangiogenic properties of silver nanoparticles. *Biomaterials* 2009;30:6341–50.
- [128] Khan MAM, Kumar S, Ahmed M, Alrokayan SA, Alsahl MS. Structural and thermal studies of silver nanoparticles and electrical transport study of their thin films. *Nanoscale Research Letters* 2011;6:434–41.
- [129] Chen D, Qiao X, Qiu X, Chen J. Synthesis and electrical properties of uniform silver nanoparticles for electronic applications. *Journal of Materials Science* 2009;44:1076–81.
- [130] Xu R, Wang D, Zhang J, Li Y. Shape-dependent catalytic activity of silver nanoparticles for the oxidation of styrene. *Science in China, Series B: Chemistry* 2006;1:888–93.
- [131] Naderi S, Ghaderi A, Solaymani S, Golzan MM. Structural, optical and thermal properties of silver colloidal nanoparticles. *The European Physical Journal Applied Physics* 2012;58:20401–4.
- [132] Feng QL, Wu J, Chen GQ, Cui FZ, Kim TN, Kim JO. A mechanistic study of the antibacterial effect of silver ions on *Escherichia coli* and *Staphylococcus aureus*. *Journal of Biomedical Materials Research* 2000;52:662–8.
- [133] Alexander S, Klabunde KJ, George MR, Christopher MS. Biocidal activity of nanocrystalline silver powders and particles. *Langmuir* 2008;24:7457–64.
- [134] Nanda A, Saravanan M. Biosynthesis of silver nanoparticles from *Staphylococcus aureus* and its antimicrobial activity against MRSA and MRSE. *Nanomedicine: Nanotechnology, Biology and Medicine* 2009;5:452–6.
- [135] Kim KJ, Sung WS, Suh BK, Moon SK, Choi JS, Kim JG. Antifungal activity and mode of action of silver nano-particles on *Candida albicans*. *Biometals* 2009;22:235–42.
- [136] Pinto DB, Shukla S, Perkas N, Gedanken A, Sarid R. Inhibition of Herpes Simplex Virus Type 1 infection by silver nanoparticles capped with mercaptoethane sulfonate. *Bioconjugate Chemistry* 2009;20:1497–502.
- [137] Lara HH, Ayala-Nunez NV, Turrent LI, Padilla CR. Mode of antiviral action of silver nanoparticles against HIV-1. *Journal of Nanobiotechnology* 2010;8:1–9.
- [138] Lu L, Sun RW, Chen R, Hui CK, Ho CM, Luk JM, et al. Silver nanoparticles inhibit hepatitis B virus replication. *Antiviral Therapy* 2008;13:253–62.
- [139] Sun L, Singh AK, Vig K, Pillai SR, Singh SR. Silver nanoparticles inhibit replication of respiratory syncytial virus. *Journal of Biomedicine and Biotechnology* 2008;4:149–58.
- [140] Elechiguerra JL, Burt JL, Morones JR, Camacho-Bragado A, Gao X, Lara HH, et al. Interaction of silver nanoparticles with HIV-1. *Journal of Nanobiotechnology* 2005;3:6–10.
- [141] Rogers JV, Parkinson CV, Choi YW, Speshock JL, Hussain SM. A preliminary assessment of silver nanoparticles inhibition of monkey pox virus plaque formation. *Nanoscale Research Letters* 2008;3:129–33.
- [142] Frederix F, Friedt JM, Choi KH, Laureyn W, Campitelli A, Mondelaers D, et al. Biosensing based on light absorption of nanoscaled gold and silver particles. *Analytical Chemistry* 2003;75: 6894–900.
- [143] Frens G. Controlled nucleation for the regulation of the particle size in monodisperse gold suspensions. *Nature Physical Science* 1973;241:20–2.
- [144] Sun Y, Mayers B, Xia Y. Metal nanostructures with hollow interiors. *Advanced Materials* 2003;15:641–6.
- [145] Pyrassopoulos S, Niarhos D, Nounous G, Boukos N, Zafiropolou I, Tzitzios V. Synthesis and self organization of Au nanoparticles. *Nanotechnology* 2007;18, 485604/1–4.
- [146] Kundu S, Panigrahi S, Praharaj S, Basu S, Ghosh SK, Pal A, et al. Anisotropic growth of gold clusters to gold nanocubes under UV irradiation. *Nanotechnology* 2007;18, 075712/1–7.
- [147] Kundu S, Peng L, Liang H. A new route to obtain high-yield multiple-shaped gold nanoparticles in aqueous solution using microwave radiation. *Inorganic Chemistry* 2008;47:6344–52.
- [148] Elghanian R, Storhoff JJ, Mucic RC, Letsinger RL, Mirkin CA. Selective colorimetric detection of polynucleotides based on the distance-dependent optical properties of gold nanoparticles. *Science* 1997;277:1078–80.
- [149] Jain PK, Huang X, El-sayed IH, El-sayed MA. Noble metals on the nanoscale: optical and photothermal properties and some applications in imaging, sensing, biology, and medicine. *Accounts of Chemical Research* 2008;41:1578–86.
- [150] Zhang Y, Schwartzberg AM, Xu K, Gu C, Zhang JZ. Electrical and thermal conductivities of gold and silver nanoparticles in solutions and films and electrical field enhanced surface-enhanced raman scattering (SERS). *Proceedings of SPIE* 2005;5929:592912.
- [151] Mukherjee P, Bhattacharya R, Wang P, Wang L, Basu S, Nagy JA, et al. Antiangiogenic properties of gold nanoparticles. *Clinical Cancer Research* 2005;11:3530–4.
- [152] Chen X, Zhao DY, Zhao LZ, An YL, Ma RJ, Shi LQ, et al. Optic and catalytic properties of gold nanoparticles tuned by homopolymers. *Science in China, Series B: Chemistry* 2009;52:1372–81.
- [153] Greget R, Nealon GL, Vileno B, Turek PP, Meny C, Ott F, et al. Magnetic properties of gold nanoparticles: a room-temperature quantum effect. *ChemPhysChem* 2012;13:3092–7.
- [154] Ortega MA, Rodriguez L, Castillo J, Piscitelli V, Fernandez A, Echevarria L. Thermo-optical properties of gold nanoparticles in colloidal systems. *Journal of Optics A: Pure and Applied Optics* 2008;10, 104024/1–4.
- [155] Gil-Tomas J. Lethal photosensitisation of *Staphylococcus aureus* using a toluidine blue O-tiopronin–gold nanoparticles conjugate. *Journal of Materials Chemistry* 2007;17:3739–46.
- [156] Perni S. The antimicrobial properties of light-activated polymers containing methylene blue and gold nanoparticles. *Biomaterials* 2009;30:89–93.
- [157] Gu H, Ho PL, Tong E, Wang L, Xu B. Presenting vancomycin on nanoparticles to enhance antimicrobial activities. *Nano Letters* 2003;3:1261–3.
- [158] Giancivincenzo PD, Marradi M, Martinez-Avila OM, Bedoya LM, Alcamí J, Penades S. Gold nanoparticles capped with sulfate-ended ligands as anti-HIV agents. *Bioorganic and Medicinal Chemistry Letters* 2010;20:2718–21.
- [159] Deboutiere PJ, Roux S, Vocanson F, Billotey C, Beul O, Favre-Reguillon A, et al. Design of gold nanoparticles for magnetic resonance imaging. *Advanced Functional Materials* 2006;16:2330–9.
- [160] Huang X, Qian W, El-Sayed IH, El-Sayed MA. The potential use of the enhanced nonlinear properties of gold nanospheres in photothermal cancer therapy. *Lasers in Surgery and Medicine* 2007;39:747–53.
- [161] Huang X, El-Sayed IH, Qian W, El-Sayed MA. Cancer cell imaging and photothermal therapy in the near-infrared region by using gold nanorods. *Journal of the American Chemical Society* 2006;128:2115–20.
- [162] Huang X, Jain PK, El-Sayed IH, El-Sayed MA. Gold nanoparticles: interesting optical properties and recent applications in cancer diagnostics and therapy. *Nanomedicine (Lond)* 2007;2:681–93.
- [163] Agarwal A, Huang SW, O'Donnell M, Day KC, Day M, Kotov N, et al. Targeted gold nanorod contrast agent for prostate cancer detection by photoacoustic imaging. *Journal of Applied Physics* 2007;102, 064701/1–4.
- [164] Plueddemann EP, Clark HA, Nelson LE, Hoffman KR. Silane coupling agents for reinforced plastics. *Mod Plast* 1962;39:135.
- [165] Owen MJ. Coupling agents: chemical bonding at interfaces. *Adhesion Science and Engineering* 2002;2:403–31.
- [166] Plueddemann EP. Adhesion through silane coupling agents. *Journal of Adhesion* 1970;2:184–201.
- [167] Uyanik M. Synthesis and characterization of TiO₂ nanostars. PhD Thesis. Saarland University, Saarbrücken, 2008, 199 pp.
- [168] Lin F. Preparation and characterization of polymer TiO₂ nanocomposites via In-situ polymerization. Master Thesis. University of Waterloo, Ontario, Canada, 2006, 160 pp.
- [169] Guo YK, Wang MY, Zhang HQ, Liu GD, Zhang LQ, Qu XW. The surface modification of nanosilica, preparation of nanosilica/acrylic core-shell composite latex, and its application in toughening PVC matrix. *Journal of Applied Polymer Science* 2008;107:2671–80.
- [170] Kim KJ, White JL. Silica surface modification using different aliphatic chain length silane coupling agents and their effects on

- silica agglomerate size and processability. *Composite Interfaces* 2002;9:541–56.
- [171] Ukaji E, Furusawa T, Sato M, Suzuki N. The effect of surface modification with silane coupling agent on suppressing the photo-catalytic activity of fine TiO₂ particles as inorganic UV filter. *Applied Surface Science* 2007;254:563–9.
- [172] Tang E, Liu H, Sun L, Zheng E, Cheng G. Fabrication of zinc oxide/poly(styrene) grafted nanocomposite latex and its dispersion. *European Polymer Journal* 2007;43:4210–8.
- [173] Sabzi M, Mirabedini SM, Zohuriaan-Mehr J, Atai M. Surface modification of TiO₂ nano-particles with silane coupling agent and investigation of its effect on the properties of polyurethane composite coating. *Progress in Organic Coatings* 2009;65:222–8.
- [174] Wang C, Mao H, Wang C, Fu S. Dispersibility and hydrophobicity analysis of titanium dioxide nanoparticles grafted with silane coupling agent. *Industrial and Engineering Chemistry Research* 2011;50:11930–4.
- [175] Zhao J, Milanova M, Warmoeskerken MMCG, Dutschk V. Surface modification of TiO₂ nanoparticles with silane coupling agents. *Colloids and Surfaces A* 2012;413:273–9.
- [176] Ma SR, Shi LY, Feng X, Yu WJ, Lu B. Graft modification of ZnO nanoparticles with silane coupling agent KH570 in mixed solvent. *Journal of Shanghai University* 2005;12:278–82.
- [177] Shen X, Gui S, Lin B. Surface organic modification of Fe₃O₄ nanoparticles by silane-coupling agents. *Rare Metals* 2006;25:426–30.
- [178] Truong TL, Larsen A, Holme B, Diplas S, Hansen FK, Roots J, et al. Dispersion of silane-functionalized alumina nanoparticles in syndiotactic polypropylene. *Surface and Interface Analysis* 2010;42:1046–9.
- [179] Guo Z, Pereira T, Choi O, Wang Y, Hahn HT. Surface functionalized alumina nanoparticle filled polymeric nanocomposites with enhanced mechanical properties. *Journal of Materials Chemistry* 2006;16:2800–8.
- [180] Mallakpour S, Barati A. Efficient preparation of hybrid nanocomposite coatings based on poly(vinyl alcohol) and silane coupling agent modified TiO₂ nanoparticles. *Progress in Organic Coatings* 2011;71:391–8.
- [181] Rong MZ, Zhang MQ, Zheng YX, Zeng HM, Walter R, Friedrich K. Structure-property relationships of irradiation grafted nano inorganic particle filled polypropylene composites. *Polymer* 2001;42:167–83.
- [182] Tran Y, Auroy P. Synthesis of polystyrene sulfonate brushes. *Journal of the American Chemical Society* 2001;123:3644–54.
- [183] Mansky P, Liu Y, Huang E, Russell TP, Hawker C. Controlling polymer-surface interactions with random copolymer brushes. *Science* 1997;275:1458–60.
- [184] Prucker O, Ruhe J. Synthesis of poly(styrene) monolayers attached to high surface area silica gels through self assembled monolayers of azo initiators. *Macromolecules* 1998;31:592–601.
- [185] Kickelbick G. Concepts for the incorporation of inorganic building blocks into organic polymers on a nanoscale. *Progress in Polymer Science* 2003;28:83–114.
- [186] Tsubokawa N, Kogure A, Sone Y. Grafting of polyesters from ultrafine inorganic particles: copolymerization of epoxides with cyclic acid anhydrides initiated by COOK groups introduced onto the surface. *Journal of Polymer Science Part A: Polymer Chemistry* 1995;28:1923–33.
- [187] von Werne T, Patten TE. Atom transfer radical polymerization from nanoparticles: A tool for the preparation of well-defined hybrid nanostructures and for understanding the chemistry of controlled “living” radical polymerizations from surfaces. *Journal of the American Chemical Society* 2001;123:7497–505.
- [188] Rong MZ, Ji QL, Zhang MQ, Friedrich K. Graft polymerization of vinyl monomers onto nanosized alumina particles. *European Polymer Journal* 2002;38:1573–82.
- [189] Sidorenko A, Minko S, Gafitjukh G, Voronov S. Radical polymerization initiated from a solid substrate: grafting from the surface of an ultrafine powder. *Macromolecules* 1999;32:4539–43.
- [190] Wang X, Song X, Lin M, Wang H, Zhao Y, Zhong W, et al. Surface initiated graft polymerization from carbon-doped TiO₂ nanoparticles under sunlight illumination. *Polymer* 2007;48:5834–8.
- [191] Tsubokawa N, Hayashi S, Nishimura J. Grafting of hyperbranched polymers onto ultrafine silica: postgraft polymerization of vinyl monomers initiated by pendant azo groups of grafted polymer chains on the surface. *Progress in Organic Coatings* 2002;44:69–74.
- [192] Shirai Y, Kawatsura K, Tsubokawa N. Graft polymerization of vinyl monomers from initiating groups introduced onto polymethylsiloxane-coated titanium dioxide modified with alcoholic hydroxyl groups. *Progress in Organic Coatings* 1999;36:217–24.
- [193] Fan X, Lin L, Messersmith PB. Surface-initiated polymerization from TiO₂ nanoparticle surfaces through a biomimetic initiator: A new route toward polymer-matrix nanocomposites. *Composites Science and Technology* 2006;66:1195–201.
- [194] Rong MZ, Zhang MQ, Wang HB, Zeng HM. Surface modification of magnetic metal nanoparticles through irradiation graft polymerization. *Applied Surface Science* 2002;200:76–93.
- [195] Yokoyama R, Suzuki S, Shirai K, Yamauchi T, Tsubokawa N, Tsuchimochi M. Preparation and properties of biocompatible polymer-grafted silica nanoparticles. *European Polymer Journal* 2006;42:3221–9.
- [196] Tang E, Cheng G, Ma X, Pang X, Zhao Q. Surface modification of zinc oxide nanoparticle by PMAA and its dispersion in aqueous system. *Applied Surface Science* 2006;252:5227–32.
- [197] Hong RY, Qian JZ, Cao JX. Synthesis and characterization of PMMA grafted ZnO nanoparticles. *Powder Technology* 2006;163:160–8.
- [198] Bach LG, Islam Md R, Kim JT, Seo SY, Lim KT. Encapsulation of Fe₃O₄ magnetic nanoparticles with poly(methyl methacrylate) via surface functionalized thiol-lactam initiated radical polymerization. *Applied Surface Science* 2012;258:2959–66.
- [199] Shirai Y, Tsubokawa N. Grafting of polymers onto ultrafine inorganic particle surface: graft polymerization of vinyl monomers initiated by the system consisting of trichloroacetyl groups on the surface and molybdenum hexacarbonyl. *Reactive and Functional Polymers* 1997;32:153–60.
- [200] Liu P, Wang T. Poly(hydroethyl acrylate) grafted from ZnO nanoparticles via surface-initiated atom transfer radical polymerization. *Current Applied Physics* 2008;8:66–70.
- [201] Shin Y, Lee D, Lee K, Ahn KH, Kim B. Surface properties of silica nanoparticles modified with polymers for polymer nanocomposite applications. *Journal of Industrial and Engineering Chemistry* 2008;14:515–9.
- [202] Murray CB, Norris D, Bawendi MG. Synthesis and characterization of nearly monodisperse CdE (E = sulfur, selenium, tellurium) semiconductor nanocrystallites. *Journal of the American Chemical Society* 1993;115:8706–15.
- [203] Greenham NC, Peng X, Alivisatos AP. Charge separation and transport in conjugated-polymer/semiconductor-nanocrystal composites studied by photoluminescence quenching and photoconductivity. *Physical Review B* 1996;54:17628–37.
- [204] Lu Z, Yin Y. Colloidal nanoparticle clusters: functional materials by design. *Chemical Society Reviews* 2012;41:6874–87.
- [205] Huynh WU, Dittmer JJ, Libby WC, Whiting GL, Alivisatos AP. Controlling the morphology of nanocrystal-polymer composites for solar cells. *Advanced Functional Materials* 2003;13:73–9.
- [206] Celik D, Krueger M, Veit C, Schleiermacher HF, Zimmermann B, Allard S, et al. Performance enhancement of CdSe nanorod-polymer based hybrid solar cells utilizing a novel combination of post-synthetic nanoparticle surface treatments. *Solar Energy Materials and Solar Cells* 2012;98:433–40.
- [207] Zhou Y, Riehle FS, Yuan Y, Schleiermacher HF, Niggemann M, Urban GA, et al. Improved efficiency of hybrid solar cells based on non-ligand-exchanged CdSe quantum dots and poly(3-hexylthiophene). *Applied Physics Letters* 2010;96, 013304/1–3.
- [208] Liao HC, Chen SY, Liu DM. In-situ growing CdS single-crystal nanorods via P3HT polymer as a soft template for enhancing photovoltaic performance. *Macromolecules* 2009;42:6558–63.
- [209] Hu W, Gao S, Prasad PN, Wang J, Xu J. Employing photoassisted ligand exchange technique in layered quantum dot LEDs. *Journal of Nanomaterials* 2012, 719169/1–5.
- [210] Lokteva I, Radychev N, Witt F, Borchert H, Parisi J, Kolny-Olesiak J. Surface treatment of CdSe nanoparticles for application in hybrid solar cells: the effect of multiple ligand exchange with pyridine. *Journal of Physical Chemistry C* 2010;114:12784–91.
- [211] Wang F, Banerjee D, Liu Y, Chen X, Liu X. Upconversion nanoparticles in biological labeling, imaging, and therapy. *Analyst* 2010;135:1839–54.
- [212] Sato K, Kondo S, Tsukada M, Ishigaki T, Kamiya H. Influence of solid fraction on the optimum molecular weight of polymer dispersants in aqueous TiO₂ nanoparticle suspensions. *Journal of the American Ceramic Society* 2007;90:3401–6.
- [213] Palmqvist L, Holmberg K. Dispersant adsorption and viscoelasticity of alumina suspensions measured by quartz crystal microbalance with dissipation monitoring and in situ dynamic rheology. *Langmuir* 2008;24:9989–96.

- [214] Nsib F, Ayed N, Chevalier Y. Dispersion of hematite suspensions with sodium polymethacrylate dispersants in alkaline medium. *Colloids and Surfaces A* 2006;286:17–26.
- [215] Pileni MP. The role of soft colloidal templates in controlling the size and shape of inorganic nanocrystals. *Nature Materials* 2003;2:145–50.
- [216] Murray CB, Kagan CR, Bawendi MG. Synthesis and characterization of monodisperse nanocrystals and close-packed nanocrystal assemblies. *Annual Review of Materials Science* 2000;30: 545–610.
- [217] Feldmann C. Polyol-mediated synthesis of nanoscale functional materials. *Advanced Functional Materials* 2003;13:101–7.
- [218] Hong RY, Li JH, Chen LL, Liu DQ, Li HZ, Zheng Y, et al. Synthesis, surface modification and photocatalytic property of ZnO nanoparticles. *Powder Technology* 2009;189:426–32.
- [219] Kobayashi M, Matsuno R, Otsuka H, Takahara A. Precise surface structure control of inorganic solid and metal oxide nanoparticles through surface-initiated radical polymerization. *Science and Technology of Advanced Materials* 2006;7:617–28.
- [220] Tang E, Cheng G, Ma X. Preparation of nano-ZnO/PMMA composite particles via grafting of the copolymer onto the surface of zinc oxide nanoparticles. *Powder Technology* 2006;161:209–14.
- [221] Tristantini D, Slamet Mustikasari, Widuri R. Modification of TiO₂ nanoparticle with PEG and SiO₂ for anti-fogging and self-cleaning application. *International Journal of Engineering & Technology* 2011;11:80–5.
- [222] Wang DS, Wang YH, Li XY, Luo QZ, An J, Yue HX. Sunlight photocatalytic activity of polypyrrrole-TiO₂ nanocomposites prepared by in situ method. *Catalysis Communications* 2008;9:1162–6.
- [223] Zhu YF, Xu SB, Jiang L, Pan KL, Dan Y. Synthesis and characterization of polythiophene/titanium dioxide composites. *Reactive and Functional Polymers* 2008;68:1492–8.
- [224] Li XY, Wang DS, Cheng GX, Luo QZ, An J, Wang YH. Preparation of polyaniline-modified TiO₂ nanoparticles and their photocatalytic activity under visible light illumination. *Applied Catalysis B* 2008;81:267–73.
- [225] Song L, Zeng X, Zhang X. Photocatalytic activities of TiO₂ modified by poly(fluorene-co-bithiophene) under visible light. In: 2010 International Conference on Biology, Environment and Chemistry, International Proceedings of Chemical, Biological and Environmental Engineering. 2010. p. 364–7.
- [226] Inbaraj BS, Tsai TU, Chen BH. Synthesis, characterization and antibacterial activity of superparamagnetic nanoparticles modified with glycol chitosan. *Science and Technology of Advanced Materials* 2012;13, 015002/1–8.
- [227] Galindo BR, Durate ML, Urbina PB, Fernandez RO, Valdes SS. Surface modification of ZnO nanoparticles. *Materials Science Forum* 2010;644:61–4.
- [228] Conde J, Doria G, Baptista P. Noble metal nanoparticles applications in cancer. *Journal of Drug Delivery* 2012, 751075/1–12.
- [229] Sperling RA, Parak WJ. Surface modification, functionalization and bioconjugation of colloidal inorganic nanoparticles. *Philosophical Transactions of the Royal Society A* 2010;368:1333–83.
- [230] Zhang Y, Kohler N, Zhang M. Surface modification of superparamagnetic nanoparticles and their intracellular uptake. *Biomaterials* 2002;23:1553–61.
- [231] Sun C, Lee JSH, Zhang M. Magnetic nanoparticles in MR imaging and drug delivery. *Advanced Drug Delivery Reviews* 2008;60: 1252–65.
- [232] Cheyne RW, Smith TAD, Trembleau L, McLaughlin AC. Synthesis and characterisation of biologically compatible TiO₂ nanoparticles. *Nanoscale Research Letters* 2011;6:423–8.
- [233] Kohler N, Sun C, Wang J, Zhang MQ. Methotrexate-modified superparamagnetic nanoparticles and their intracellular uptake into human cancer cells. *Langmuir* 2005;21:8858–64.
- [234] Kohler N, Sun C, Fichtenthaler A, Gunn J, Fang C, Zhang MQ. Methotrexate immobilized poly(ethylene glycol) magnetic nanoparticles for MR imaging and drug delivery. *Small* 2006;2:785–92.
- [235] Chertok B, David AE, Yang VC. Polyethyleneimine modified iron oxide nanoparticles for brain tumor drug delivery using magnetic targeting and intra-carotid administration. *Biomaterials* 2010;31:6317–24.
- [236] Shen T, Weissleder R, Papisov M, Bogdanov Jr A, Brady TJ. Monocrystalline iron oxide nanocompounds (MION): physicochemical properties. *Magnetic Resonance in Medicine* 1993;29:599–604.
- [237] Josephson L, Tung CH, Moore A, Weissleder R. High-efficiency intracellular magnetic labeling with novel superparamagnetic-Tat peptide conjugates. *Bioconjugate Chemistry* 1999;10:186–91.
- [238] Wunderbaldinger P, Josephson L, Weissleder R. Tat peptide directs enhanced clearance and hepatic permeability of magnetic nanoparticles. *Bioconjugate Chemistry* 2002;13:264–8.
- [239] Schellenberger EA, Bogdanov Jr A, Hogemann D, Tait J, Weissleder R, Josephson L. AnnexinV-CLIO a nanoparticle for detecting apoptosis by MRI. *Molecular Imaging* 2002;1:102–7.
- [240] Celis R, Hermosin MC, Cornejo J. Heavy metal adsorption by functionalized clays. *Environmental Science and Technology* 2000;34:4593–9.
- [241] Lagadic IL, Mitchell MK, Payne BD. Highly effective adsorption of heavy metal ions by a thiol-functionalized magnesium phyllosilicate clay. *Environmental Science and Technology* 2001;35: 984–90.
- [242] Brown J, Mercier L, Pinnavaia TJ. Selective adsorption of Hg²⁺ by thiol-functionalized nanoporous silica. *Chemical Communications* 1999;1:69–70.
- [243] Yoshitake H, Yokoi T, Tatsumi T. Adsorption behavior of arsenate at transition metal cations captured by amino-functionalized mesoporous silica. *Chemistry of Materials* 2003;15:1713–21.
- [244] Takafuji M, Ide S, Ihara H, Xu Z. Preparation of poly(1-vinylimidazole)-grafted magnetic nanoparticles and their application for removal of metal ions. *Chemistry of Materials* 2004;16:1977–83.
- [245] Pu X, Jiang Z, Hu B, Wang H. γ -MPTMS modified nanometer-sized alumina micro-column separation and preconcentration of trace amounts of Hg, Cu, Au and Pd in biological, environmental and geological samples and their determination by inductively coupled plasma mass spectrometry. *Journal of Analytical Atomic Spectrometry* 2004;19:984–9.
- [246] Yang D, Paul B, Xu W, Yuan Y, Liu E, Ke X, et al. Alumina nanofibers grafted with functional groups: a new design in efficient sorbents for removal of toxic contaminants from water. *Water Research* 2010;44:741–50.
- [247] Pang Y, Zeng G, Tang L, Zhang Y, Liu Y, Lei X, et al. PEI-grafted magnetic porous powder for highly effective adsorption of heavy metal ions. *Desalination* 2011;281:278–84.
- [248] Hussain F, Hojjati M, Okamoto M, Gorga RE. Review article: polymer-matrix nanocomposites, processing, manufacturing, and application: an overview. *Journal of Composite Materials* 2006;40:1511–75.
- [249] Brinker C, Scherer G. Sol-gel science: physics and chemistry of sol-gel science processing. Toronto: Academic Press; 1990. p. 2–10.
- [250] Hsieh GH, Kuo WJ, Jeng RJ. Microstructural and morphological characteristics of PS-SiO₂ nanocomposites. *Polymer* 2000;41: 2813–25.
- [251] Song KY, Crivello JV, Ghoshal R. Synthesis and photoinitiated cationic polymerization of organic inorganic hybrid. *Chemistry of Materials* 2001;13:1932–42.
- [252] Silveira KF, Yoshida IVP, Nunes SP. Phase separation in PMMA/silica sol-gel systems. *Polymer* 1995;36:1425–34.
- [253] Nunes SP, Peinemann KV, Ohlrogge K, Alpers A, Keller M, Pires ATN. Membranes of poly(ether imide) and nanodispersed silica. *Journal of Membrane Science* 1999;157:219–26.
- [254] Suzuki F, Onozato K, Kurokawa Y. A Formation of compatible poly(vinyl alcohol)/alumina gel composite and its properties. *Journal of Applied Polymer Science* 1990;39:371–81.
- [255] Sengupta R, Bandyopadhyay A, Sabharwal S, Chaki TK, Bhowmick AK. Polyamide 6,6/in situ silica hybrid nanocomposites by sol-gel technique: synthesis, characterization and properties. *Polymer* 2005;46:3343–54.
- [256] Hsieh GH, Chen JK, Liu YL. Synthesis and characterization of nanocomposite of polyimide-silica hybrid from nonaqueous sol-gel process. *Journal of Applied Polymer Science* 2000;76: 1608–18.
- [257] Wu CS. In situ polymerization of titanium isopropoxide in polycaprolactone: properties and characterization of the hybrid nanocomposites. *Journal of Applied Polymer Science* 2004;92:1749–57.
- [258] Du T, Song H, Illegbusi OJ. Sol-gel derived ZnO/PVP nanocomposite thin film for superoxide radical sensor. *Materials Science and Engineering C* 2007;27:414–20.
- [259] Hu Q, Marand E. In situ formation of nanosized TiO₂ domains within poly(amide-imide) by a sol-gel process. *Polymer* 1999;40:4833–43.
- [260] Garcia M, van Vliet G, Cate ten MGJ, Chavez F, Norder B, Kooi B, et al. Large-scale extrusion processing and characterization of hybrid nylon-6/SiO₂ nanocomposites. *Polymers for Advanced Technologies* 2004;15:164–72.

- [261] Ou Y, Yang F, Yu Z. A new conception on the toughness of nylon 6/silica nanocomposite prepared via *in situ* polymerization. *Journal of Polymer Science Part B: Polymer Physics* 1998;36:789–95.
- [262] Ou Y, Yang F, Chen J. Interfacial interaction and mechanical properties of nylon 6 potassium titanate composites prepared by *in-situ* polymerization. *Journal of Applied Polymer Science* 1997;64:2317–22.
- [263] Guan C, Lu CL, Cheng YR, Song SY, Yang BA. Facile one-pot route to transparent polymer nanocomposites with high ZnS nanoparticle contents via *in situ* bulk polymerization. *Journal of Materials Chemistry* 2009;19:617–21.
- [264] Jiang J. Ultrasonic-assisted synthesis of PMMA/ $\text{Ni}_{0.5}\text{Zn}_{0.5}\text{Fe}_2\text{O}_4$ nanocomposite in mixed surfactant system. *European Polymer Journal* 2007;43:1724–8.
- [265] Cheng Y, Lu C, Lin Z, Liu Y, Guan C, Lu H, et al. Preparation and properties of transparent bulk polymer nanocomposites with high nanoparticle contents. *Journal of Materials Chemistry* 2008;18:4062–8.
- [266] Dzunuzovic E, Jeremic K, Nedeljkovic JM. In situ radical polymerization of methyl methacrylate in a solution of surface modified TiO_2 and nanoparticles. *European Polymer Journal* 2007;43:3719–26.
- [267] Yari M, Sedaghat S. In situ synthesis and characterization of conducting metal–polyaniline nanocomposites. *Journal of Physical and Theoretical Chemistry of Islamic Azad University of Iran* 2009;5:189–93.
- [268] Park SS, Bernet N, Roche DLS, Hahn HT. Processing of iron oxide–epoxy vinyl ester nanocomposites. *Journal of Composite Materials* 2003;37:465–76.
- [269] Evora VMF, Shukla A. Fabrication, characterization, and dynamic behavior of polyester/TiO₂ nanocomposites. *Materials Science and Engineering A* 2003;361:358–66.
- [270] Aymonier C, Bortzmeyer D, Thomann R, Mulhaupt R. Poly(methyl methacrylate)/palladium nanocomposites: synthesis and characterization of the morphological, thermomechanical, and thermal properties. *Chemistry of Materials* 2003;15:4874–8.
- [271] Chaichana E, Jongsomjit B, Praserttham P. Effect of nano-SiO₂ particle size on the formation of LLDPE/SiO₂ nanocomposite synthesized via the *in situ* polymerization with metallocene catalyst. *Chemical Engineering Science* 2007;62:899–905.
- [272] Zhang MQ, Rong MZ, Friedrich K. Processing and properties of nonlayered nanoparticles reinforced thermoplastic composites. In: Nalwa HS, editor. *Handbook of organic–inorganic hybrid materials and nanocomposites*. Stevenson Ranch: American Scientific Publishers; 2003. p. 113–50.
- [273] van Zyl WE, Garcia M, Schrauwen BAG, Kooi BJ, De Hosson JTM, Verweij H. Hybrid polyamide/silica nanocomposites: synthesis and mechanical testing. *Macromolecular Materials and Engineering* 2002;287:106–10.
- [274] Li JH, Hong RY, Li MY, Li HZ, Zheng Y, Ding J. Effect of ZnO nanoparticles on the mechanical and antibacterial properties of polyurethane coatings. *Progress in Organic Coatings* 2009;64:504–9.
- [275] Wang YJ, Kim D. Crystallinity morphology, mechanical properties and conductivity study of *in situ* formed PVDF/LiClO₄/TiO₂ nanocomposite polymer electrolytes. *Electrochimica Acta* 2007;52:3181–9.
- [276] Hong RY, Feng B, Liu G, Wang S, Li HZ, Ding JM, et al. Preparation and characterization of Fe₃O₄/polystyrene composite particles via inverse emulsion polymerization. *Journal of Alloys and Compounds* 2009;476:612–8.
- [277] Zhang SW, Zhou SX, Weng YM, Wu LM. Synthesis of SiO₂/polystyrene nanocomposite particles via miniemulsion polymerization. *Langmuir* 2005;21:2124–8.
- [278] Wang YQ, Li YP, Zhang RY, Huang L, He WW. Synthesis and characterization of nanosilica/polyacrylate composite latex. *Polymer Composites* 2006;27:282–8.
- [279] Caris CHM, Kuijpers RPM, van Herk AM, German AL. Kinetics of (co)polymerization at the surface of inorganic submicron particles in emulsion-like systems. *Makromolekulare Chemie, Macromolekulare Symposium* 1990;35/36:535–48.
- [280] Erdem B, Sudol ED, Dimonie VL, El-Aasser MS. Encapsulation of inorganic particles via miniemulsion polymerization, II. Preparation and characterization of styrene miniemulsion droplets containing TiO₂ particles. *Journal of Polymer Science Part A: Polymer Chemistry* 2000;38:4431–40.
- [281] Erdem N, Cireli AA, Erdogan UH. Flame retardancy behaviours and structural properties of polypropylene/nano-SiO₂ composite textile filaments. *Journal of Applied Polymer Science* 2009;111:2085–91.
- [282] Zhao H, Li RKY. A study on the photo-degradation of zinc oxide (ZnO) filled polypropylene nanocomposites. *Polymer* 2006;47:3207–17.
- [283] Kim SH, Ahn SH, Hirai T. Crystallization kinetics and nucleation activity of silica nanoparticle-filled poly(ethylene 2,6-naphthalate). *Polymer* 2003;44:5625–34.
- [284] Li S, Lin MM, Toprak MS, Kim DK, Muhammed M. Nanocomposites of polymer and inorganic nanoparticles for optical and magnetic applications. *Nano Review* 2010;1, 5214-doi:10.3402/nano.v1i0.5214/1–19.
- [285] Hong JI, Cho KS, Chung CI, Schadler LS, Siegel RW. Retarded cross-linking in ZnO–low density polyethylene nanocomposites. *Journal of Materials Research* 2002;17:940–3.
- [286] Ma CCM, Chen YJ, Kuan HC. Polystyrene nanocomposite materials—preparation, mechanical, electrical and thermal properties, and morphology. *Journal of Applied Polymer Science* 2006;100:508–15.
- [287] Chan CM, Wu JS, Li JX, Cheung YK. Polypropylene/calcium carbonate nanocomposites. *Polymer* 2002;43:2981–92.
- [288] Bhimaraj P, Burris DL, Action J, Sawyer WG, Toney CG, Siegel RW. Effect of matrix morphology on the wear and friction behavior of alumina nanoparticle/Poly(ethylene) terephthalate composites. *Wear* 2005;258:1437–43.
- [289] Wang S, Yang S, Yang C, Li Z, Wang J, Ge W. Poly(N-vinylcarbazole) (PVK) photoconductivity enhancement induced by doping with CdS nanocrystals through chemical hybridization. *Journal of Physical Chemistry B* 2000;104:11853–8.
- [290] Sheng W, Kim S, Lee J, Kim S, Jensen K, Bawendi M. In-situ encapsulation of quantum dots into polymer microspheres. *Langmuir* 2006;22:3782–90.
- [291] Park JH, Park OO. Photorefractive properties in poly(N-vinylcarbazole)/CdSe nanocomposites through chemical hybridization. *Applied Physics Letters* 2006;89, 193101/1–3.
- [292] Fusheng P, Cheng Q, Jia H, Jiang Z. Facile approach to polymer–inorganic nanocomposite membrane through a biomineralization-inspired process. *Journal of Membrane Science* 2010;357:171–7.
- [293] Pomogailo AD, Kestelman VN. Chemical methods of metal–polymer nanocomposite production. In: Pomogailo AD, Kestelman VN, editors. *Metallopolymer nanocomposites*. Springer series in materials science, vol. 81. Berlin: Springer; 2005. p. 135–236.
- [294] Balan L, Burget D. Synthesis of metal/polymer nanocomposite by UV-radiation curing. *European Polymer Journal* 2006;42:3180–9.
- [295] Eisa WH, Abdel-Moneam YK, Shabaka AA, Hosam AEM. In situ approach induced growth of highly monodispersed Ag nanoparticles within free standing PVA/PVP films. *Spectrochimica Acta, Part A* 2012;95:341–6.
- [296] Kanade KG, Hawaldar RR, Mulik UP, Kale BB, Amalnerkar DP. Synthesis of CdS nanocrystallites in polymer matrix: sui-generis approach. *Solid State Phenomena* 2007;119:21–6.
- [297] Suh SK, Yuet K, Hwang DK, Bong KW, Doyle PS, Hatton TA. Synthesis of nonspherical superparamagnetic particles: in situ coprecipitation of magnetic nanoparticles in microgels prepared by stop-flow lithography. *Journal of the American Chemical Society* 2012;134:7337–43.
- [298] Porel S, Venkatram N, Rao DN, Radhakrishnan TP. In situ synthesis of metal nanoparticles in polymer matrix and their optical limiting applications. *Journal of Nanoscience and Nanotechnology* 2007;7:1887–92.
- [299] Khan MT, Kaur A, Dhawan SK, Chand S. In-Situ growth of cadmium telluride nanocrystals in poly(3-hexylthiophene) matrix for photovoltaic application. *Journal of Applied Physics* 2011;110, 044509/1–7.
- [300] Zhou S, Su Q, Li X, Weng J. A novel *in situ* synthesis of dicalcium phosphate dehydrate nanocrystals in biodegradable polymer matrix. *Materials Science and Engineering A* 2006;430:341–5.
- [301] Nakao Y. Preparation and characterization of noble metal solid sols in poly (methyl methacrylate). *Journal of the Chemical Society, Chemical Communications* 1993;10:826–8.
- [302] Yanagihara N. Reduction and agglomeration of silver in the course of formation of silver nano cluster in poly(methyl methacrylate). *Chemistry Letters* 1998;27:305–6.
- [303] Zhou Y, Hao LY, Zhu YR, Hu Y, Chen ZY. A novel ultraviolet irradiation technique for fabrication of polyacrylamide–metal (M = Au, Pd) nanocomposites at room temperature. *Journal of Nanoparticle Research* 2001;3:379–83.
- [304] Khanna PK, Singh N, Charan S, Viswanath AK. Synthesis of Ag/polyaniline nanocomposite via an *in situ* photo-redox mechanism. *Materials Chemistry and Physics* 2005;92:214–9.

- [305] Tamboli MS, Kulkarni MV, Patil RH, Gade WN, Navale SC, Kale BB. Nanowires of silver-polyaniline nanocomposite synthesized via *in situ* polymerization and its novel functionality as an antibacterial agent. *Colloids and Surfaces B* 2012;92:35–41.
- [306] Wang K, Chen L, Wu J, Toh ML, He C, Yee AF. Epoxy nanocomposites with highly exfoliated clay: mechanical properties and fracture mechanisms. *Macromolecules* 2005;38:788–800.
- [307] Lee H, Lin L. Waterborne polyurethane/clay nanocomposites: novel effects of the clay and its interlayer ions on the morphology and physical and electrical properties. *Macromolecules* 2006;39:6133–41.
- [308] Zhang X, Simon LC. In situ polymerization of hybrid polyethylene-alumina nanocomposites. *Macromolecular Materials and Engineering* 2005;290:573–83.
- [309] Jiang L, Lam YC, Tam KC, Chua TH, Sim GW, Ang LS. Strengthening acrylonitrile-butadiene-styrene (ABS) with nano-sized and micron-sized calcium carbonate. *Polymer* 2005;46:243–52.
- [310] Zhang M, Singh R. Mechanical reinforcement of unsaturated polyester by Al_2O_3 nanoparticles. *Materials Letters* 2004;58:408–12.
- [311] Wang Y, Lim S, Luo JL, Xu ZH. Tribological and corrosion behaviors of Al_2O_3 /polymer nanocomposite coatings. *Wear* 2006;260:976–83.
- [312] Zhang Z, Yang JL. Creep resistant polymeric nanocomposites. *Polymer* 2004;45:3481–5.
- [313] Chisholm N, Mahfuz H, Rangari VK, Jeelani S. Fabrication and mechanical characterization of carbon/SiC-epoxy nanocomposites. *Composite Structures* 2005;67:115–24.
- [314] Ng CB, Schadler LS, Siegel RW. Synthesis and mechanical properties of TiO_2 -epoxy nanocomposites. *Nanostructured Materials* 1999;12:507–10.
- [315] Rong MZ, Zhang MQ, Liu H, Zeng HM, Wetzel B, Friedrich K. Microstructure and tribological behavior of polymeric nanocomposites. *Industrial Lubrication and Tribology* 2001;53:72–7.
- [316] Schwartz CJ, Bahadur S. Studies on the tribological behavior and transfer film-counterface bond strength for polyphenylene sulphide filled with nanoscale alumina particles. *Wear* 2000;237:261–73.
- [317] Siegel RW, Chang SK, Ash BJ, Stone JAPM, Doremus RW, Schadler LS. Mechanical behavior of polymer and ceramic matrix nanocomposites. *Scripta Materialia* 2001;44:2061–4.
- [318] Yuwono AH, Liu B, Xue J, Wang J, Elim HI, Ji W, et al. Controlling the crystallinity and nonlinear optical properties of transparent TiO_2 -PMMA nanohybrids. *Journal of Materials Chemistry* 2004;14:2978–87.
- [319] Khrenov V, Klapper M, Koch M, Mullen K. Surface functionalized ZnO particles designed for the use in transparent nanocomposites. *Macromolecular Chemistry and Physics* 2005;206:95–101.
- [320] Li S, Toprak MS, Jo YS, Dobson J, Kim DK, Muhammed M. Bulk synthesis of transparent and homogeneous polymeric hybrid materials with ZnO quantum dots and PMMA. *Advanced Materials* 2007;19:4347–52.
- [321] Ritzhaupt-Kleissl E, Bohm J, Haubelt J, Hanemann T. Thermoplastic polymer nanocomposites for applications in optical devices. *Materials Science and Engineering C* 2006;26:1067–71.
- [322] Althues H, Potschke P, Kim GM, Kaskel S. Structure and mechanical properties of transparent ZnO/PBDMA nanocomposites. *Journal of Nanoscience and Nanotechnology* 2009;9:2739–45.
- [323] Sun DZ, Sue HJ. Tunable ultraviolet emission of ZnO quantum dots in transparent poly(methyl methacrylate). *Applied Physics Letters* 2009;94:253106/1–3.
- [324] Du XW, Fu YS, Sun J, Han X, Liu J. Complete UV emission of ZnO nanoparticles in a PMMA matrix. *Semiconductor Science and Technology* 2006;21:1202–6.
- [325] Vollath D, Szabo DV. Synthesis and properties of nanocomposites. *Advanced Engineering Materials* 2004;6:117–27.
- [326] Wang ZG, Zu XT, Xiang X, Yu HJ. Photoluminescence from TiO_2/PMMA nanocomposite prepared by gamma radiation. *Journal of Nanoparticle Research* 2006;8:137–9.
- [327] Vollath D, Szabo DV, Schlabach S. Oxide/polymer nanocomposites as new luminescent materials. *Journal of Nanoparticle Research* 2004;6:181–91.
- [328] Peres M, Costa LC, Neves A, Soares MJ, Monteiro T, Esteves AC, et al. A green-emitting CdSe/poly(butyl acrylate) nanocomposite. *Nanotechnology* 2005;16:1969–73.
- [329] Yang Y, Li YQ, Fu SY, Xiao HM. Transparent and light-emitting epoxy nanocomposites containing ZnO quantum dots as encapsulating materials for solid state lighting. *Journal of Physical Chemistry C* 2008;112:10553–8.
- [330] Xiong HM, Xu Y, Ren QG, Xia YY. Stable aqueous ZnO at polymer core/shell nanoparticles with tunable photoluminescence and their application in cell imaging. *Journal of the American Chemical Society* 2008;130:7522–3.
- [331] Althues H, Henle J, Kaskel S. Functional inorganic nanofillers for transparent polymers. *Chemical Society Reviews* 2007;36:1454–65.
- [332] Lu C, Guan C, Liu Y, Cheng Y, Yang B. PbS/polymer nanocomposite optical materials with high refractive index. *Chemistry of Materials* 2005;17:2448–54.
- [333] Lu C, Cheng Y, Liu Y, Liu F, Yang B. A facile route to ZnS -polymer nanocomposite optical materials with high nanoparticle content via γ -ray irradiation initiated bulk polymerization. *Advanced Materials* 2006;18:1188–92.
- [334] Kyrianiotou-Leodidou T, Margraf P, Caseri W, Suter UW, Walther P. Polymer sheets with a thin nanocomposite layer acting as a UV filter. *Polymers for Advanced Technologies* 1997;8:505–12.
- [335] Chau J LH, Tung CT, Lin YM, Li AK. Preparation and optical properties of titania/epoxy nanocomposite coatings. *Materials Letters* 2008;62:3416–8.
- [336] Wang H, Xu P, Zhong W, Shen L, Du Q. Transparent poly(methyl methacrylate)/silica/zirconia nanocomposites with excellent thermal stabilities. *Polymer Degradation and Stability* 2005;87:319–27.
- [337] Sarwar MI, Zulfiqar S, Ahmad Z. Polyamide-silica nanocomposites: mechanical, morphological and thermomechanical investigations. *Polymer International* 2008;57:292–6.
- [338] Chandra A, Turng LS, Gopalan P, Rowell RM, Gong S. Study of utilizing thin polymer surface coating on the nanoparticles for melt compounding of polycarbonate/alumina nanocomposites and their optical properties. *Composites Science and Technology* 2008;68:768–76.
- [339] Ziolo RF, Giannelis EP, Weinstein BA, Ohoro MP, Ganguly BN, Mehrotra V, et al. Matrix-mediated synthesis of nanocrystalline gamma- Fe_2O_3 : a new optically transparent magnetic material. *Science* 1992;257:219–23.
- [340] Ziolo RF, Giannelis EP, Shull RD. Matrix-mediated synthesis and properties of nanostructured materials. *Nanostructured Materials* 1993;3:85–92.
- [341] Jarjayes O, Fries PH, Bidan G. Magnetic properties of fine maghemite particles in an electroconducting polymer matrix. *Journal of Magnetism and Magnetic Materials* 1994;137:205–18.
- [342] Zhan J, Tian G, Jiang L, Wu Z, Wu D, Yang X, et al. Superparamagnetic polyimide/ γ - Fe_2O_3 nanocomposite films: preparation and characterization. *Thin Solid Films* 2008;516:6315–20.
- [343] Guo Z, Shin K, Karki AB, Young DP, Kaner RB, Hahn HT. Fabrication and characterization of iron oxide nanoparticles filled polypyrrole nanocomposites. *Journal of Nanoparticle Research* 2009;11:1441–52.
- [344] Su SJ, Kuramoto N. Processable polyaniline-titanium dioxide nanocomposites: effect of titanium dioxide on the conductivity. *Synthet Metal* 2000;114:147–53.
- [345] Mo TC, Wang HW, Chen SY, Yeh YC. Synthesis and dielectric properties of polyaniline/titanium dioxide nanocomposites. *Ceramics International* 2008;34:1767–71.
- [346] Ma D, Hugener TA, Siegel RW, Christerson A, Martensson E, Onneby C, et al. Influence of nanoparticle surface modification on the electrical behavior of polyethylene nanocomposites. *Nanotechnology* 2005;16:724–31.
- [347] Singha S, Thomas MJ. Dielectric properties of epoxy nanocomposites. *IEEE Transactions on Dielectrics & Electrical Insulation* 2008;15:12–23.
- [348] Ray SS, Okamoto M. Polymer/layered silicate nanocomposite: a review from preparation to processing. *Progress in Polymer Science* 2003;28:1539–41.
- [349] Chen CH, Jin JY, Yen FS. Preparation and characterization of epoxy/ γ -alumina oxide nanocomposites. *Composites Part A: Applied Science and Manufacturing* 2009;40:463–8.
- [350] Omrani A, Simon LC, Rostami AA. The effects of alumina nanoparticle on the properties of an epoxy resin system. *Materials Chemistry and Physics* 2009;114:145–50.
- [351] Kang S, Hong SI, Choe CR, Park M, Rim S, Kim J. Preparation and characterization of epoxy composites filled with functionalized nanosilica particles obtained via sol-gel process. *Polymer* 2001;42:879–87.
- [352] Wu T, Ke Y. Melting crystallization and optical behaviors of poly(ethylene terephthalate)-silica/polystyrene nanocomposite films. *Thin Solid Films* 2007;515:5220–6.
- [353] Laachachi A, Leroy E, Cochez M, Ferriol M, Cuesta JML. Use of oxide nanoparticles and organoclays to improve thermal stability and

- fire retardancy of poly(methyl methacrylate). *Polymer Degradation and Stability* 2005;89:344–52.
- [354] Rhee SH, Choi JY. Preparation of a bioactive poly(methyl methacrylate)/silica nanocomposite. *Journal of the American Ceramic Society* 2002;85:1318–20.
- [355] Camargo P, Satyanarayana K, Wypych F. Nanocomposites: synthesis, structure, properties and new application opportunities. *Materials Research* 2009;12:1–39.
- [356] Yang C, Li H, Xiong D, Cao Z. Hollow polyaniline/Fe₃O₄ microsphere composites: Preparation, characterization, and applications in microwave absorption. *Reactive and Functional Polymers* 2009;69:137–44.
- [357] Zhu Y, Kaskel S, Ikoma T, Hanagata N. Magnetic SBA-15/poly(N-isopropylacrylamide) composite: preparation, characterization and temperature-responsive drug release property. *Microporous and Mesoporous Materials* 2009;123:107–12.
- [358] Masotti A, Pitta A, Ortaggi G, Corti M, Innocenti C, Lascialfari A, et al. Synthesis and characterization of polyethylenimine-based iron oxide composites as novel contrast agents for MRI. *Magnetic Resonance Materials in Physics, Biology and Medicine* 2009;22:77–87.
- [359] Hashimoto M, Takadama H, Mizuno M, Kokubo T. Enhancement of mechanical strength of TiO₂/high-density polyethylene composites for bone repair with silane-coupling treatment. *Materials Research Bulletin* 2006;41:515–24.
- [360] Emamifar A, Kadivar M, Shahedi M, Solaimanianzad S. Effect of nanocomposite packaging containing Ag and ZnO on inactivation of *Lactobacillus plantarum* in orange juice. *Food Control* 2011;22:408–13.
- [361] Sanchez C, Julian B, Belleville P, Popall M. Applications of hybrid organic–inorganic nanocomposites. *Journal of Materials Chemistry* 2005;15:3559–92.